FIELDS AND INPUT ADMITTANCE OF A FLANGED COAXIAL ANTENNA EXCITED BY A TEM WAVE

by

Abdulmagid Abdussalam Aburwein

A Thesis Submitted to the Faculty of the

DEPARTMENT OF ELECTRICAL ENGINEERING

In Partial Fulfillment of the Requirements
For the Degree of

MASTER OF SCIENCE

In the Graduate College

THE UNIVERSITY OF ARIZONA

1 9 7 7

STATEMENT BY AUTHOR

This thesis has been submitted in partial fulfillment of requirements for an advanced degree at The University of Arizona and is deposited in the University Library to be made available to borrowers under rules of the Library.

Brief quotations from this thesis are allowable without special permission, provided that accurate acknowledgment of source is made. Requests for permission for extended quotation from or reproduction of this manuscript in whole or in part may be granted by the head of the major department or the Dean of the Graduate College when in his judgment the proposed use of the material is in the interests of scholarship. In all other instances, however, permission must be obtained from the author.

SIGNED: 

APPROVAL BY THESIS DIRECTOR

This thesis has been approved on the date shown below:

Allen Q. Howard Jr.

ALLEN Q. HOWARD, JR.
Professor of
Electrical Engineering

21 January 1977
Date

ACKNOWLEDGMENTS

I wish to take this opportunity to thank Dr. A. Q. Howard for the tremendous amount of support which he provided in his various capacities as an adviser. I also thank my wife, Saadat, for her cooperation and patience, without which this work would have been more difficult.

TABLE OF CONTENTS

LIST OF ILLUSTRATIONS

LIST OF ILLUSTRATIONS--Continued

ABSTRACT

This thesis deals with the boundary-value problem of an annular slot aperture antenna driven by a coaxial guide. The aperture is assumed to lie in an infinitely large conducting metal sheet. No restrictions are made on the aperture size in the analysis. The input to the antenna is a TEM polarized wave. The mode match method is used to derive a matrix equation for the TMon mode amplitude in the guide. All the matrix elements which are numerical integrals are considered. Special techniques are carefully developed to evaluate the integrals, since their proper evaluation is the key factor in the accuracy of the solution. The effect of 30 higher order modes on the input admittance, the operture fields, and the far field pattern is calculated and plotted. The edge behavior is derived to include TMon modes when $n > 30$. It is also shown how this condition can be used for correcting the truncation errors.

CHAPTER 1

INTRODUCTION

The annular aperture antenna is a classical problem in electromagnetic theory. Many authors realized its importance not only because of its widely applicable omniazimuthal radiation pattern as a radiator but also as a coaxial feeding element for any flush-mounted antenna system. It was noted by Chang (1970) that studying its input admittance and the near field distributions are essential to the overall system's frequency sensitivity and the breakdown performance that are, in turn, prime considerations in the design of high power UHF communication systems.

One of the important early papers on this problem was written by Levine and Papas (1951). Their paper was mainly concerned with variational methods for calculating the input equivalent circuit parameters in closed form. They considered the case where only the principle mode propagates in the coaxial region. In 1958, Cohn and Flesher derived an integral equation for the transverse magnetic mode amplitude intensity in the upper half sphere region, and successive approximations method is used to solve it. Again, small aperture (compared to the wave length of the

operating frequency) is assumed and all the higher TMon mode amplitudes in the guide region were set to zero as the first approximation. The field patterns, as expected, did not include any lobes that might be offered by the beyond cutoff TMon modes in the guide region. The same formulation and solution of the integral equation was done by Fitzgerrell et al. (1970) for the case of a small annular slot antenna buried under a dielectric. Higher order modes in the guide region were considered up to two beyond cutoff in their analysis of the input aperture impedance.

In 1970 Chang considered the aperture width to be much less than the inner coaxial guide radius and the wave length. He derived closed form expressions for the input admittance and the aperture field distributions using conformal mapping to solve the aperture field integral equation indirectly. The first five higher order modes were considered and the rest were estimated by the edge behavior. Irzinski (1975) used the mode matching technique, which we will discuss later in this chapter, and developed a matrix equation for the TMon mode amplitudes in the guide region. He also considered small aperture approximation to evaluate the integrals constituting the matrix equation in closed form. He neglected all of the off-diagonal elements of the matrix.

From the previous discussion one can see that the problem was never considered when the aperture is comparable with a wave length, which can be possible at high frequencies. The last author neglected the non-diagonal elements, which found to be comparable to the diagonal elements, especially when n and m are small, even when a small aperture is assumed.

In this thesis, we will consider a complete analysis of the problem, regardless of the aperture size or the operating frequency. We will also include all the matrix elements in the matrix equation derived in the next chapter.

In Chapter 2, the problem is formulated. From Figure 1, the geometry of the structure can be identified as a junction plane at z = 0 separating region 1 and region 2. Each of these regions belongs to a separable coordinate system. The first step in formulating the problem is to determine the fields in both regions to satisfy Maxwell's equations and boundary conditions separately. Fields in region 1 are written as a summation of all the modes existing in the guide with two unknowns, Γ_o (the voltage reflection coefficient of the TEM mode) and T_n (the TMon [to z] mode amplitude in the guide). A summation is expected due to the discrete eigen values in the guide region. On the other hand, fields in region 2 assume integration of all the TM(to z) modes present in z > 0, which is again expected due

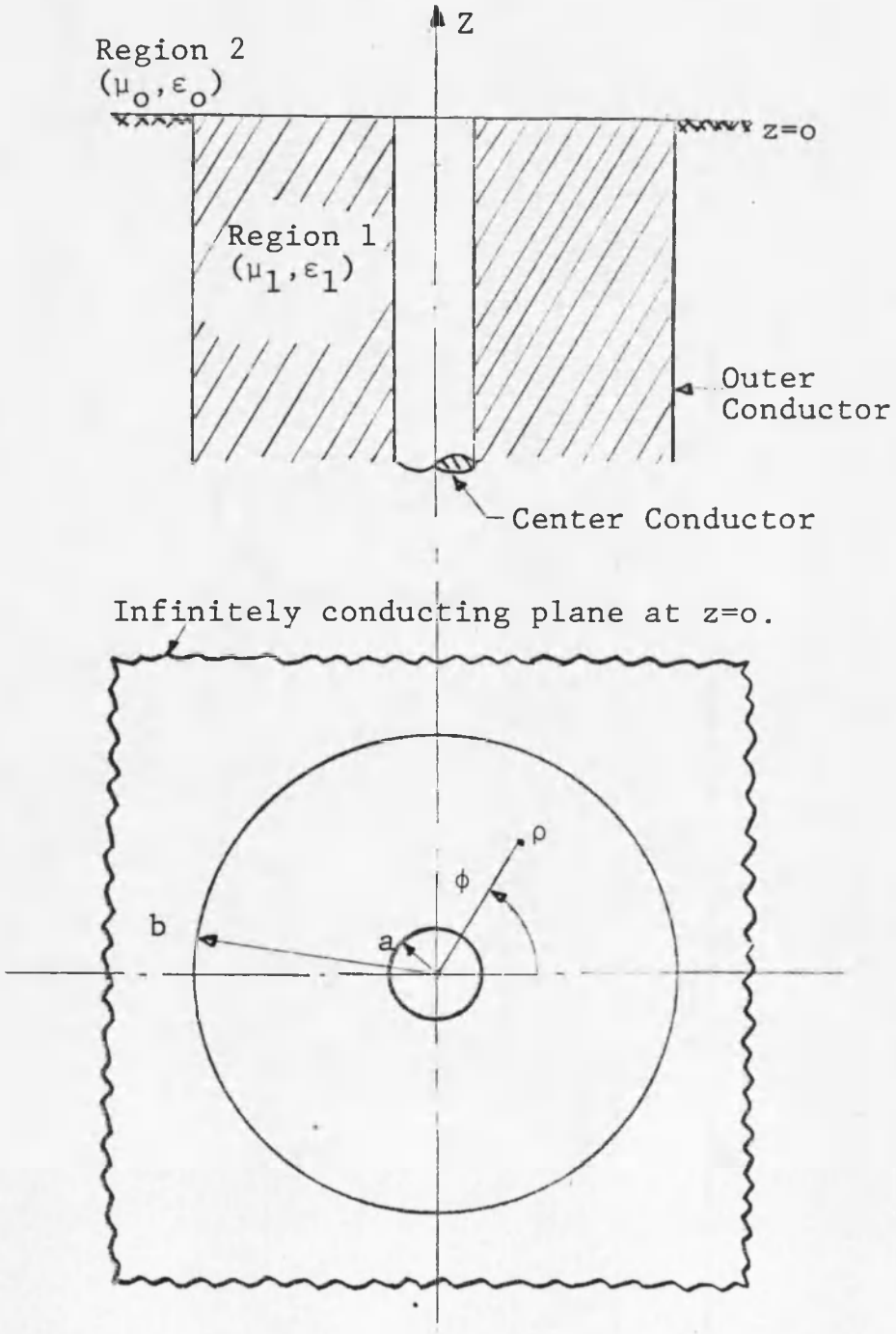

Figure 1. The geometry of the annular aperture antenna.

to the continuum of the eigen values in that region. $B(\alpha)$ (the TM [to z] mode amplitude intensity) is unknown in field expressions of region 2. The second step is to apply the continuity condition of the tangential components of the electric and magnetic fields at the aperture. This procedure along with the orthogonality properties of mode expansion functions, leads to an infinite set of linear simultaneous equations for Tn. This method of formulating the problem is called the mode match method. The mode match method is often a powerful tool when solving boundary value problems identfied as a junction of two or more separable regions. This method, though, has the disadvantage of the necessity of building an efficient numerical scheme to account for the truncation errors. In this case, this was done in regard to the integrals constituting the matrix equation in Chapter 3.

In Chapter 4, we analyze the edge behavior of the electric field at the aperture. This is a good tool to account for considering only a matrix equation of order N instead of an infinite one. The latter is clearly impossible to solve.

In Chapter 5, results are briefly discussed and suggestions for future work are presented in the conclusion section.

CHAPTER 2

THE THEORY OF THE PROBLEM

As shown in Figure 1, the geometry is divided into two regions. Region 1 is the guide region filled with the perfect dielectric ($\sigma = 0$) of a magnetic permeability μ_1, and an electric permitivity ε_1. In region 1, $z \leq 0$. Region 2 is the upper half of free space ($z \geq 0$) of permeability μ_o and permitivity ε_o.

The assumptions to be considered in solving this problem are:

1. The ground metal plane ($z = 0$, $\rho \geq b$) is of infinite conductivity (has zero ohmic losses) and extends for $\rho \geq b$ infinitely.
2. The time dependence is $\exp(i\omega t)$ where ω is the angular frequency.
3. All fields are azimuthally symmetric ($\partial/\partial\psi = 0$).
4. The input to the antenna is a TEM wave travelling in the positive z-direction. It has an amplitude T_0 (volts), and a voltage reflection coefficient Γ_0 due to the discontinuity at $z = 0$.

Fields in Region 1

The incident TEM wave excites higher order modes at the aperture. Due to the azimuthal symmetry ($\partial/\partial\psi = 0$),

the excited modes have only $E_{z_1}(\rho,z)$, $E_{\rho_1}(\rho,z)$ and $H_{\rho_1}(\rho,z)$ components. These components constitute an infinite number of TM(to z) modes travelling in the negative z-direction with $e^{Y_n z}$ on dependance. Y_n is either positive real which gives the evanscent modes, or positive imaginary which gives the propagating modes.

Maxwell's Equations in Region 1

In a source-free homogeneous region Maxwell's equations in the frequency domain are:

$$-\bar{\nabla}x\bar{E} = \hat{Z}_1\bar{H}, \quad \bar{\nabla}x\bar{H} = \hat{y}_1\bar{E}, \quad \bar{\nabla}\cdot\bar{E} = 0, \text{ and } \quad \bar{\nabla}\cdot\bar{H} = 0$$

The notation is as in Harrington (1961) with $\hat{z}_1 = i\omega\mu_1$, and $\hat{y}_1 = i\omega\varepsilon_1$. $\bar{E}$ and $\bar{H}$ are the electric and the magnetic field intensity vectors respectively. In view of the divergenceless character of $\bar{E}$ and $\bar{H}$ we can express the fields in terms of a magnetic vector potential $\bar{A}$, in terms of an electric vector potential $\bar{F}$ or we can even express part of the field in terms of $\bar{A}$ and part in terms of $\bar{F}$.

Hence let $\bar{H} = \bar{\nabla} \times \bar{A}$ (2.1)

$\bar{\nabla} \times (\bar{E} + \hat{Z}_1\bar{A}) = 0$

Any curl-free vector is the gradient of some scalar function ϕ.

Hence:

$$\bar{E} + \hat{Z}_1\bar{A} = -\bar{\nabla}\phi$$

Where ϕ is an electric scalar potential.

To obtain the equation for $\bar{A}$, we have:

$$\bar{\nabla} \times \bar{\nabla} \times \bar{A} = \bar{\nabla}(\bar{\nabla}\cdot\bar{A}) - \bar{\nabla}^2\bar{A} = \hat{y}_1\bar{E}$$

or

$$(\bar{\nabla}^2 + K_1^2)\bar{A} = 0 \qquad (2.2)$$

Where $K_1^2 = -\hat{Z}_1\hat{y}_1 = \omega^2\mu_1\varepsilon_1$

In equation (2.2) we were free to choose:

$$\bar{\nabla}\cdot\bar{A} = -\hat{y}_1\phi$$

We conclude that the magnetic potential vector obeys the homogeneous Helmholtz equation. An expression for the electric field intensity in terms of $\bar{A}$ is,

$$\bar{E} = -\hat{Z}\bar{A} + \hat{y}_1^{-1}\,\bar{\nabla}(\bar{\nabla}\cdot\bar{A}) \qquad (2.3)$$

In general, for TM(to z) we choose $\bar{A}$ such that the z-component of $\bar{H}$ vanishes. This leads us to choose

$$\bar{A} = \hat{u}_z A_{zn} e^{Y_n Z}$$

Where only the nth TM(to z) mode is considered. $\hat{u}_z$ is the unit vector in the positive z-direction.

Considering only the z-components of equation (2.2), we have

$$(\bar{\nabla}^2 + K_1^2)A_{zn}e^{Y_n z} = 0$$

If $\xi_n^2 = K_1^2 + Y_n^2$, we have

$$\frac{1}{\rho}\frac{\partial}{\partial\rho}(\rho\frac{\partial}{\partial\rho}A_{zn}) + \xi_n^2 A_{zn} = 0 \qquad (2.4)$$

Equation (2.4) is the Bessel's equation of a zero order, and its solution is:

$$A_{zn} = C_n J_o(\xi_n\rho) + D_n Y_o(\xi_n\rho) \qquad (2.5)$$

Where C_n and D_n are arbitrary constants depending on n.
$J_o(x)$ is the Bessel's function of a zero order.
$Y_o(x)$ is the Neumann function of a zero order.

From equations (2.3) and (2.5), we can write the z-components of the electric field intensity respectively as:

$$E_z(\rho, z)\Big|_{\text{due to TM}_{on}} = (\frac{Y_n^2}{\hat{y}_1} - \hat{Z}_1)A_{zn}e^{Y_n Z} = E_{zn}(\rho, z) \qquad (2.6)$$

$$E_\rho(\rho,z)\Big|_{\text{due to } TM_{on}} = \frac{Yn}{\hat{y}_1}\frac{\partial}{\partial\rho}A_{zn}e^{Y_n z} = E_{\rho n}(\rho,z) \tag{2.7}$$

Applying the boundary condition $E_{zn}(\rho,z) = 0$ to equation (2.6), we get:

$$E_{zn}(\rho,z) = \frac{D_n\xi_n^2}{\hat{y}_1 J_o(\xi_n a)}Q_o(\xi_n\rho)e^{Y_n z}$$

Where

$$Q_o(\xi_n\rho) = J_o(\xi_n a)Y_o(\xi_n\rho) - Y_o(\xi_n a)J_o(\xi_n\rho)$$

If we let $T_n = D_n\xi_n^2/\hat{y}_1 J_o(\xi_n a)$ (volts/meter), we have

$$E_{zn}(\rho,z) = T_n Q_o(\xi_n\rho)e^{Y_n z}$$

If we apply the boundary condition $E_{zn}(\rho,z) = 0$, we get the eigen function equation which defines the eigen values ξ_n's:

$$J_o(\xi_n a)Y_o(\xi_n b) = Y_o(\xi_n a)J_o(\xi_n b)$$

From equation (2.7), we can write:

$$E_{\rho n}(\rho,z) = \frac{y_n}{\xi_n} T_n Q_o'(\xi_n\rho) e^{Y_n z}$$

Where;

$$Q_o'(\xi_n\rho) = \frac{\partial}{\partial \xi_n \rho} Q_o(\xi_n\rho) = Y_o(\xi_n a)\ J_1(\xi_n\rho) -$$

$$- J_o(\xi_n a)\ Y_1(\xi_n\rho)$$

Finally, using equation (2.1), we can write the ϕ-component of $\bar{H}$ for the nth TM(to z) mode as:

$$H_{\phi n}(\rho,z) = \frac{-i\omega\varepsilon_1}{\xi_n} T_n Q_o'(\xi_n\rho) e^{Y_n z}$$

If we define the characteristic impedance of region 1 as $\eta_1 = \sqrt{\frac{\mu_1}{\varepsilon_1}}$, then the TEM wave components of $\bar{E}$ and $\bar{H}$ are:

$$E_{\rho_{TEM}}(\rho,z) = \frac{T_o}{\rho} (e^{-ik_1 z} + \Gamma_o e^{ik_1 z})$$

And,

$$H_{\phi_{TEM}}(\rho,z) = \frac{T_o}{\rho\eta_1} (e^{-ik_1 z} - \Gamma_o e^{ik_1 z})$$

To get the total fields in region 1, summation of an infinite number of TM(to z) modes and superimposing the TEM field components yields:

$$E_{z_1}(\rho,z) = \sum_{n=1}^{\infty} T_n Q_o(\xi_n\rho) e^{Y_n z} \qquad (2.8)$$

$$E_{\rho_1}(\rho,z) = \frac{T_o}{\rho}(e^{-ik_1 z} + \Gamma_o e^{ik_1 z}) + \sum_{n=1}^{\infty} \frac{Y_n}{\xi_n} T_n Q_o'(\xi_n \rho) \cdot$$

$$\cdot\ e^{Y_n z} \qquad (2.9)$$

$$H_{\phi_1}(\rho,z) = \frac{T_o}{\rho \eta_1}(e^{-ik_1 z} - \Gamma_o e^{ik_1 z}) - \sum_{n=1}^{\infty} \frac{i\omega\varepsilon_1}{\xi_n}$$

$$x\ T_n Q_o'(\xi_n \rho) e^{Y_n z} \qquad (2.10)$$

The subscript 1 denotes the region $z \leq 0$. Similar expressions to equations (2.8), (2.9) and (2.10) appeared in Levine and Papas (1951), Cohn and Flesher (1958), Fitzgerrell et al. (1970), and Irzinski (1975).

Fields in Region 2

TEM waves are not present in this region due to the absence of the center conductor that supports it. Fields in region 2 are excited by the TM(to z) circularly symmetric waves from region 1. Thus only outward circularly symmetric TM(to z) modes propagate in this region.

Figure 2 shows the assumed geometry of region 2 made by Cohn and Flesher (1958). Region 2 is defined as the limit ρ_o goes to infinity. If similar expressions to the TM mode fields in region 1 are assumed for region 2 with a

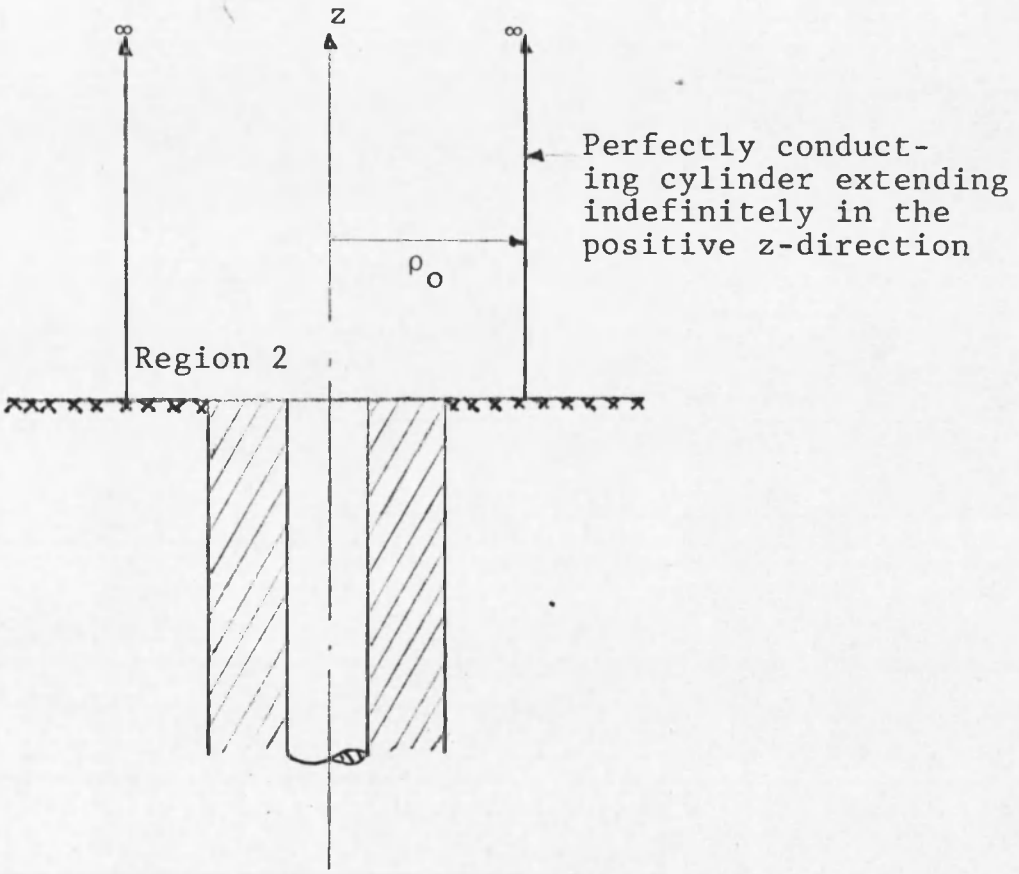

Figure 2. The assumed geometry of region 2.

new wave number $K_o = \frac{2\pi}{\omega\sqrt{\mu_o\varepsilon_o}}$, and let ρ_o go to infinity, the discrete eigenvalues ξ_n's become a real continuous variable of integration α going from 0 to ∞. Also, an unknown $B(\alpha)$ (volts/meter) is introduced to represent the TM(to z) mode amplitude intensity in region 2. Assuming $e^{-i\psi(\alpha)z}$ z-dependance we can write the total fields in region 2 as:

$$E_{z_2}(\rho,z) = \int_o^\infty B(\alpha)J_o(\alpha\rho)e^{-i\psi(\alpha)z}d\alpha \qquad (2.11)$$

$$E_{\rho_2}(\rho,z) = \int_o^\infty \frac{i\psi(\alpha)}{\alpha}B(\alpha)J_1(\alpha\rho)e^{-i\psi(\alpha)z}d\alpha \qquad (2.12)$$

$$H_{\phi_2}(\rho,z) = \int_o^\infty \frac{i\omega\varepsilon_o}{\alpha}B(\alpha)J_1(\alpha\rho)e^{-i\psi(\alpha)z}d\alpha \qquad (2.13)$$

Where

$$\psi^2(\alpha) = K_o^2 - \alpha^2$$

$$\psi(\alpha) = (K_o^2 - \alpha^2)^{1/2} \quad \text{for} \quad K_o \geq \alpha$$

$$= -i(\alpha^2 - K_o^2)^{1/2} \quad \text{for} \quad \alpha \geq K_o$$

The Neumann functions are not present in the field expressions because they are singular at $\rho = o$.

Again, similar expressions for fields in region 2 appeared in the same papers mentioned in the previous section of this chapter.

Mode Matching in the Aperture

The geometry of the antenna shown in Figure 1 is very suitable for the mode matching technique. At the aperture ($z = o$ and $a \leq \rho \leq b$), both the tangential components of $\bar{E}$ and $\bar{H}$ are continuous. This can be obtained from the curl equations with no surface current. These two independent boundary conditions are:

$$E_{\rho_1}(\rho,o) = E_{\rho_2}(\rho,o) \quad \text{for} \quad a \leq \rho \leq b \tag{2.14}$$

and

$$H_{\phi_1}(\rho,o) = H_{\phi_2}(\rho,o) \quad \text{for} \quad a \leq \rho \leq b \tag{2.15}$$

From equations (2.14) and (2.15), we have:

$$\frac{T_o(1+\Gamma_o)}{\rho} + \sum_{n=1}^{\infty} \frac{Y_n}{\xi_n} Q_o'(\xi_n\rho)T_n = \int_o^{\infty} \frac{i\psi(\alpha)}{\alpha} B(\alpha)J_1(\alpha\rho)d\alpha \tag{2.16}$$

$$\frac{T_o(1-\Gamma_o)}{\rho\eta_1} - \sum_{n=1}^{\infty} \frac{i\omega\varepsilon_1}{\xi_n} Q_o'(\xi_n\rho)T_n = \int_o^{\infty} \frac{i\omega\varepsilon_o}{\alpha} B(\alpha)J_1(\alpha\rho)d\alpha \tag{2.17}$$

From (2.16) and (2.17), we seek three equations to relate the three unknowns Γ_o, T_n and $B(\alpha)$. If we multiply both sides of (2.16) by $J_1(\alpha'\rho)$ and integrate from $\rho = a$ to $\rho = b$, we get:

$$T_o(1+\Gamma_o)\int_a^b J_1(\alpha'\rho)d\rho + \sum_{n=1}^{\infty} \frac{Y_n}{\xi_n} T_n \int_a^b \rho Q_o'(\xi_n\rho)J_1(\alpha'\rho)d\rho$$

$$= \int_o^\infty \rho d\rho \int_o^\infty \frac{i\psi(\alpha)B(\alpha)}{\alpha^2} \cdot J_1(\alpha\rho)J_1(\alpha'\rho)\alpha d\alpha \qquad (2.18)$$

Note that the integration over ρ in the right hand side of (2.18) takes the limits $\rho = a$ to $\rho = b$. This can be done since $E_{\rho_2}(\rho,o) = o$ for $b \geq \rho \geq a$.

From Watson (1958, p. 142), the Fourier Bessel Transform is:

$$\int_o^\infty u\, du \int_o^\infty F(R)J_\nu(uR)J_\nu(ur)RdR = F(r)$$

From Abramowitz and Stegun (1970, p. 484), we have:

$$\int_z^z \{(K^2 - \ell^2)t - \frac{(\mu^2-\nu^2)}{t}\} \beta_\mu(kt)\Omega_\nu(\ell t)dt$$

$$= z\{k\beta_{\mu+1}(kz)\Omega_\nu(\ell z) - \ell\beta_\mu(kz)\Omega_{\nu+1}(\ell z)\} - (\mu-\nu)$$

$$\beta_\mu(kz)\Omega_\nu(\ell z) \qquad (2.19)$$

Where $\beta_n(y)$ and $\Omega_n(y)$ can represent any linear combination of $J_n(y)$ and $Y_n(y)$. If we use the wronksian relation $J_n(z)Y_{n+1}(z)-J_{n+1}(z)Y_n(z) = -2/\pi z$ and let $\beta_\mu(kt)$ denote $Q_o'(\xi_n\rho)$ and $\Omega_\nu(\ell t)$ denote $J_1(\alpha'\rho)$, equation (2.19) reduces to:

$$\int_a^b Q_o'(\xi_n\rho)J_1(\alpha'\rho)\rho d\rho = \frac{2\alpha' R_n(\alpha')}{\pi\xi_n(\xi_n^2-\alpha'^2)} .$$

Where;

$$R_n(\alpha) = J_o(\alpha b)\frac{J_o(\xi_n a)}{J_o(\xi_n b)} - J_o(\alpha a)$$

Knowing that $\int_a^b J_1(\alpha'\rho)d\rho = \frac{J_o(\alpha' a) - J_o(\alpha' b)}{\alpha'}$, equation (2.18) can be rewritten as:

$$\frac{i\psi(\alpha)B(\alpha)}{\alpha^2} = \frac{T_o(1+\Gamma_o)}{\alpha}[J_o(\alpha a)-J_o(\alpha b)] + \sum_{m=1}^{\infty}\frac{2Y_m\alpha R_m(\alpha)}{\pi\xi_m^2(\xi_m^2-\alpha^2)} . \qquad (2.20)$$

For a second relation between the unknowns, let us multiply both sides of equation (2.17) by $\rho Q_o'(\xi_m\rho)$ and integrate from $\rho = a$ to $\rho = b$ yielding:

$$-\varepsilon_1 \sum_{n=1}^{\infty}\frac{T_n}{\xi_n}\int_a^b Q_o'(\xi_n\rho)Q_o'(\xi_m\rho)\rho d\rho = \frac{2\varepsilon_o}{\pi\xi_n}\int_o^{\infty}\frac{B(\alpha)R_n(\alpha)d\alpha}{(\xi_n^2-\alpha^2)} \qquad (2.21)$$

For $\beta_n(y)$ denoting any linear combination of $J_n(y)$ and $Y_n(y)$, we have the recurrence relation:

$$\frac{\partial}{\partial y}\left[y^n \beta_n(y)\right] = y^n \beta_{n-1}(y)$$

Integrating once by parts and using the above relation, we get:

$$\int_a^b Q_o'(\xi_n \rho) Q_o'(\xi_m \rho) \rho \, d\rho = \frac{\xi_n}{\xi_m} \int_a^b Q_o(\xi_n \rho) Q_o(\xi_m \rho) \rho \, d\rho$$

From Abramowitz and Stegun (1970, p. 485), we have:

$$\int_a^b t \beta_\nu(\lambda_m t) \beta_\nu(\lambda_n t) dt = \delta_{nm}\left[\frac{t^2}{2} \left\{ \left(1 - \frac{\nu^2}{\lambda_n^2 t^2}\right) \beta_\nu(\lambda_n t) + \beta_\nu'^2(\lambda_n t) \right\} \right]_a^b \qquad (2.22)$$

Where; δ_{nm} is Kronecker delta function.

$$\delta_{nm} = 0 \qquad n \neq m$$
$$= 1 \qquad n = m$$

If $\nu = 1$ or 0, equation (2.22) reduces to:

$$\int_a^b Q_o'(\xi_n \rho) Q_o'(\xi_m \rho) \rho \, d\rho = \int_a^b Q_o(\xi_n \rho) Q_o(\xi_m \rho) \rho \, d\rho$$
$$= \delta_{nm}\left[\frac{-2Z_n(a,b)}{(\pi \xi_n)^2} \right]$$

Where;

$$Z_n(a,b) = 1 - \left(J_o(\xi_n a)/J_o(\xi_n b)\right)^2 .$$

From the previous discussion, equation (2.21) becomes:

$$T_n = \frac{\pi \varepsilon_o \xi_n^2}{\varepsilon_1 Z_n(a,b)} \int_o^\infty B(\alpha) \frac{R_n(\alpha)}{(\xi_n^2 - \alpha^2)} d\alpha \qquad (2.23)$$

The final relation between Γ_o, T_n, and $B(\alpha)$ is obtained by integrating both sides of equation (2.17) over ρ, from $\rho = a$ to $\rho = b$ yielding:

$$\frac{T_o \ln (b/a)}{\eta_1} (1-\Gamma_o) = i\omega\varepsilon_o \int_o^\infty \frac{B(\alpha)}{\alpha^2} [J_o(\alpha a) - J_o(\alpha b)] d\alpha \qquad (2.24)$$

Derivation of the Matrix Equation

In this section, we derive a matrix equation for T_n. This matrix equation is to be solved numerically. A normalized (unitless) symmetrical matrix is preferable for numerical reasons. Thus, let:

$$t_n = \frac{T_n Y_n}{\pi \xi_n^2 T_o} \qquad C(\alpha) = \frac{B(\alpha)}{T_o} .$$

We now can rewrite equations (2.20), (2.23), and (2.24) as:

$$C(\alpha) = \frac{i}{\psi(\alpha)} \left[(1+\Gamma_o)(J_o(\alpha a) - J_o(\alpha b)) + \sum_{m=1}^{\infty} \frac{2\alpha^3 R_m(\alpha)}{(\xi_m^2 - \alpha^2)} t_m \right] \qquad (2.25)$$

$$t_n = \frac{\varepsilon_o Y_n}{\varepsilon_1 Z_n(a,b)} \int_o^\infty \frac{C(\alpha) R_n(\alpha)}{(\xi_n^2 - \alpha^2)} \, d\alpha \tag{2.26}$$

$$1 - \Gamma_o = \frac{i\omega \varepsilon_o \eta_1}{\ln(b/a)} \int_o^\infty \frac{C(\alpha)[J_o(\alpha a) - J_o(\alpha b)]}{\alpha^2} \, d\alpha \tag{2.27}$$

Substituting the value of $C(\alpha)$ from equation (2.25) in equation (2.26) yields:

$$t_n = \frac{\varepsilon_o Y_n}{i\varepsilon_1 Z_n(a,b)} \left[(1+\Gamma_o) P_n(a,b) + \sum_{m=1}^{\infty} 2 J_{nm}(a,b) t_m \right] \tag{2.28}$$

Where;

$$P_n(a,b) = \int_o^\infty \frac{\alpha R_n(\alpha)[J_o(\alpha a) - J_o(\alpha b)]}{\psi(\alpha)(\xi_n^2 - \alpha^2)} \, d\alpha$$

$$J_{nm}(a,b) = \int_o^\infty \frac{\alpha^3}{\psi(\alpha)} \frac{R_n(\alpha)}{(\xi_n^2 - \alpha^2)} \frac{R_m(\alpha)}{(\xi_m^2 - \alpha^2)} \, d\alpha$$

Now, let us substitute the value of $C(\alpha)$ from equation (2.25) in equation (2.27) to get:

$$1 - \Gamma_o = \frac{\omega \varepsilon_o \eta_1}{\ln(b/a)} \left[(1+\Gamma_o) I(a,b) + \sum_{m=1}^{\infty} 2 P_m(a,b) t_m \right] \tag{2.29}$$

Where;

$$I(a,b) = \int_o^\infty \frac{[J_o(\alpha a) - J_o(\alpha b)]^2}{\alpha \psi(\alpha)} \, d\alpha$$

From equations (2.28) and (2.29), we can write the matrix equation as:

$$\sum_{m=1}^{\infty} L_{nm} t_m = f_n(a,b) \tag{2.30}$$

Where;

$$L_{nm} = K(a,b)P_n(a,b)P_m(a,b) - J_{nm}(a,b) + \delta_{nm}(i\varepsilon_1 Z_n(a,b))/2\varepsilon_o Y_n \ .$$

$$f_n(a,b) = \frac{\ln(b/a)K(a,b)P_n(a,b)}{\eta_1 \omega \varepsilon_o} \ .$$

$$K(a,b) = \frac{\eta_1 \omega \varepsilon_o}{\ln(b/a)+\eta_1 \omega \varepsilon_o I(a,b)} \ .$$

The matrix equation (2.30) is to be solved numerically for t_m. It is not a difficult task to get Γ_o and $B(\alpha)$ after that.

If we let the matrices $\underset{\sim}{A}$, $\underset{\sim}{X}$, and $\underset{\sim}{B}$ represent $\{L_{nm}\}$, $\{t_m\}$, and $\{f_n(a,b)\}$ (m,n = 1,2, ..., N), respectively, we get:

$$\underset{\sim}{A} \cdot \underset{\sim}{X} = \underset{\sim}{B} \tag{2.31}$$

Let;

$$\underset{\sim}{A} = \begin{bmatrix} u_{11} & u_{12} & \cdots & u_{1N} \\ \ell_{21} & u_{22} & \cdots & u_{2N} \\ \vdots & & & \vdots \\ \ell_{N1} & & & u_{NN} \end{bmatrix}$$

Note that the infinite system (2.30) is truncated at some finite order N.

Since we are not interested in the inverse matrix of $\underset{\sim}{A}$, the so-called LU-decomposition method (Forsythe and Moler, 1967, Chapter 9) is used to solve (2.31).

Briefly the matrix $\underset{\sim}{A}$ is decomposed to two matrices, $\underset{\sim}{L}$ and $\underset{\sim}{U}$, such that $\underset{\sim}{L}\underset{\sim}{U} = \underset{\sim}{A}$. Where $\underset{\sim}{L}$ and $\underset{\sim}{U}$ take the forms:

$$\underset{\sim}{L} = \begin{bmatrix} 1 & & \\ \ell_{21} & 1 & \underset{\sim}{0} \\ \vdots & & \\ \ell_{2N} & \cdots & 1 \end{bmatrix} \quad \text{and} \quad \underset{\sim}{U} = \begin{bmatrix} u_{11} & u_{12} & \cdots & u_{1N} \\ & u_{22} & & \\ & & & \vdots \\ \underset{\sim}{0} & & & u_{NN} \end{bmatrix}$$

Solution of (2.31) is achieved by first solving $\underset{\sim}{L}\underset{\sim}{y} = \underset{\sim}{B}$ (forward elimination) and then solve $\underset{\sim}{U}\underset{\sim}{X} = \underset{\sim}{Y}$ (back substitution).

The main advantage of this method is the save of memory locations which is very desirable for N large.

CHAPTER 3

EVALUATION OF INTEGRALS AND NUMERICAL TECHNIQUES

In this chapter we will consider the integrals and prepare them for numerical evaluation.

To account for all the elements of matrix equation, we have three integrals to evaluate. They are defined in Chapter 2 as:

$$I(a,b) = \int_0^\infty \frac{[J_o(\alpha a)-J_o(\alpha b)]^2}{\alpha\psi(\alpha)}\, d\alpha = Re[I(a,b)] + iIm[I(a,b)] \ , \ i = \sqrt{-1} \ .$$

$$P_n(a,b) = \int_0^\infty \frac{\alpha[J_o(\alpha a)-J_0(\alpha b)]R_n(\alpha)}{\psi(\alpha)(\xi_n^2-\alpha^2)}\, d\alpha = Re[P_n(a,b)] + iIm[P_n(a,b)] \ .$$

$$J_{nm}(a,b) = \int_0^\infty \frac{\alpha^3}{\psi(\alpha)} \frac{R_n(\alpha)}{(\xi_n^2-\alpha^2)} \frac{R_m(\alpha)}{(\xi_m^2-\alpha^2)}\, d\alpha = Re[J_{nm}(a,b)] + iIm[J_{nm}(a,b)] \ .$$

Where $R_n(\alpha)$ is defined as:

$$R_n(\alpha) = J_o(\alpha b)J_o(\xi_n a)/J_o(\xi_n b) - J_o(\alpha a) = Q_n(\alpha)/J_o(\xi_n b) \ .$$

Thus:

$$Q_n(\alpha) = J_o(\alpha b)J_o(\xi_n a) - J_o(\alpha a)J_o(\xi_n b)$$

Where:

$$\psi(\alpha) = \sqrt{k_o^2 - \alpha^2} \qquad \text{for } k_o \geq \alpha \text{ and}$$

$$\psi(\alpha) = -i\sqrt{\alpha^2 - k_o^2} \qquad \text{for } \alpha \geq k_o \ .$$

The integral $J_{nm}(a,b)$ depends on n and m. Upon reduction $J_{nm}(a,b)$ dependence to one modal index only, an appreciable numerical evaluation time is saved. Let us define the integral $q_n(x)$ as:

$$q_n(x) = \int_o^\infty \frac{\alpha J_o(\alpha x)Q_n(\alpha)}{\psi(\alpha)(\xi_n^2-\alpha^2)}\, d\alpha \ , \ x = a \text{ or } b$$

Using the partial fraction technique, we reduce $J_{nm}(a,b)$ to:

$$J_{nm}(a,b) = \frac{\xi_n^2[h_m q_n(b) - d_m q_n(a)] - \xi_m^2[h_n q_m(b) - d_n q_m(a)]}{d_n d_m(\xi_m^2-\xi_n^2)}$$

Where: $h_n = J_o(\xi_n a)$ and $d_n = J_o(\xi_n b)$. For n = m, we can write $J_{nm}(a,b)$ as:

$$J_{nn}(a,b) = \frac{1}{d_n^2}\int_o^\infty \frac{\alpha^3}{\psi(\alpha)}\frac{Q_n^2(\alpha)}{(\xi_n^2-\alpha^2)^2}\, d\alpha$$

Note that the integral $P_n(a,b)$ reduces to:

$$P_n(a,b) = [q_n(a) - q_n(b)]/d_n \ .$$

From the previous discussion, we now have the integrals $I(a,b)$, $q_n(a)$, $q_n(b)$, and $J_{nn}(a,b)$ to evaluate. Due to the branch cut in $\psi(\alpha)$, each of these integrals has a real and an imaginary part. If we make the change of variables $\alpha = k_o \sin\theta$ for the real parts, we have:

$$\mathrm{Re}[I(a,b)] = \int_0^{\pi/2} \frac{[J_o(k_o a \sin\theta) - J_o(k_o b \sin\theta)]^2}{k_o \sin\theta} \, d\theta \tag{3.1}$$

$$\mathrm{Re}[q_n(x)] = \int_0^{\pi/2} \frac{k_o \sin\theta \, J_o(k_o x \sin\theta) Q_n(k_o \sin\theta)}{(\xi_n^2 - k_o^2 \sin^2\theta)} \, d\theta \tag{3.2}$$

$$\mathrm{Re}[J_{nn}(a,b)] = \int_0^{\pi/2} \frac{(k_o \sin\theta)^3}{d_n^2} \frac{Q_n^2(k_o \sin\theta)}{(\xi_n^2 - k_o^2 \sin^2\theta)^2} \, d\theta \tag{3.3}$$

Integrands of (3.1), (3.2), and (3.3) are smooth within the limits of integration. They do not oscillate when $\xi_n > k_o$ while they have few oscillations when $\varepsilon_n < k_o$. A Gaussian quadrature scheme of numerical integration (Abramowitz and Stegun, 1970, p. 887) is used. Forty-eight quadrature points or a 96 degree polynomial to fit the integrands gave excellent results. Both integrands of (3.2) and (3.3) are not defined at $\theta = \theta_n = \sin^{-1}(k_o/\xi_n)$, hence the first three terms of Taylor's series of $Q_o(k_o \sin\theta)$ and the expression

$\xi_n^2-k_o^2 \sin^2\theta$ around $\theta = \theta_n$ are used to approximately define the integrands for $|\theta-\theta_n| \leq 10^{-5}$.

If the change of variables $\alpha = k_o \cosh\theta$ is made for the imaginary parts of the integrals, we have:

$$\mathrm{Im}[I(a,b)] = \int_o^\infty \frac{[J_o(k_o a \cosh\vartheta)-J_o(k_o b \cosh\vartheta)]^2}{k_o \cosh\theta}\, d\theta$$

$$= \int_o^\infty f_1(\theta,a,b,k_o)\,d\theta \qquad (3.4)$$

$$\mathrm{Im}[q_n(x)] = \int_o^\infty \frac{k_o \cosh\theta J_o(k_o x \cosh\theta) Q_n(k_o \cosh\theta)}{(\xi_n^2-k_o^2\cosh^2\theta)}\, d\theta$$

$$= \int_o^\infty f_2(\theta,n,a,b,x,k_o)\,d\theta \qquad (3.5)$$

$$\mathrm{Im}[J_{nn}(a,b)] = \int_o^\infty \frac{(k_o \cosh\theta)^3}{d_n^2} \frac{Q_n^2(k_o\cosh\theta)}{(\xi_n^2-k_o^2\cosh^2\theta)^2}\, d\theta$$

$$= \int_o^\infty \frac{f_3(\theta,n,a,b,k_o)}{d_n^2}\, d\theta \qquad (3.6)$$

For non-propagating TM_{on} (to Z) modes in region 1 ($\xi_n > k_o$), we can show that (Levine and Papas, 1951; Marcuvitz, 1951):

$$\mathrm{Im}[I(a,b)] = \frac{1}{\pi k_o} \int_o^\pi [2\mathrm{Si}\{k_o(a^2+b^2-2ab\cos\phi)^{1/2}\}$$

$$- \mathrm{Si}\{2k_o a \sin(\phi/2)\}$$

$$- \mathrm{Si}\{2k_o b \sin(\phi/2)\}]d\phi \qquad (3.7)$$

Where:

$$Si(x) = \int_0^x \frac{\sin t}{t}\, dt \ .$$

Integrals (3.5) and (3.6) are evaluated numerically. For $\xi_n < k_o$ (both evanescent and propagating TM modes exist in region 1), equation (3.7) does not hold and the integral (3.4) is performed numerically too.

For large y ($y \geq 13$), $J_o(y)$ can be approximated by $(2/\pi y)^{\frac{1}{2}}\cos(y-\pi/4)$. Provided that $k_o a \cosh\theta \geq 13$, we can apply this approximation on $f_1(\theta,a,b,k_o)$, $f_2(\theta,n,a,b,x,k_o)$, and $f_3(\theta,n,a,b,k_o)$ to get:

$$f_1(\theta,a,b,k_o) \tilde{=} \frac{2}{\pi k_o^2 \cosh^2\theta}\left[\frac{\cos(k_o a \cosh\theta - \pi/4)}{\sqrt{a}} - \frac{\cos(k_o b \cosh\theta - \pi/4)}{\sqrt{b}}\right] = f_{1a}(\theta) \tag{3.8}$$

$$f_2(\theta,n,a,b,x,k_o) \tilde{=} \frac{2}{\pi\sqrt{x}(\xi_n^2 - k_o^2\cosh^2\theta)}\left[\frac{J_o(\xi_n a)}{\sqrt{b}}\{\sin(k_o(b+x)\cosh\theta) + \cos(k_o(b-x)\cosh\theta)\} - \frac{J_o(\xi_n b)}{\sqrt{a}}\{\sin(k_o(x+a)\cosh\theta) + \cos(k_o(x-a)\cosh\theta)\}\right] = f_{2a}(\theta) \tag{3.9}$$

$$f_3(\theta,n,a,b,k_o) \cong \frac{2k_o^2 \cosh^2\theta}{\pi(\xi_n^2 - k_o^2 \cosh^2\theta)^2} \left[\frac{J_o(\xi_n a)}{\sqrt{b}} \cos \right.$$

$$(k_o b \cosh\theta - \pi/4) - \frac{J_o(\xi_n b)}{\sqrt{a}} \cos$$

$$\left. (k_o a \cosh\theta - \pi/4) \right]^2 = f_{3a}(\theta) \quad (3.10)$$

Now;

$$Im[I(a,b)] \cong \int_o^{\theta_i} f_1(\theta,a,b,k_o)d\theta + \int_{\theta_i}^{\infty} f_{1a}(\theta)d\theta$$

$$= G_I(\theta_i,a,b,k_o) + G_{Ia}(\theta_i) \quad (3.11)$$

Where;

$$G_I(\theta_i,a,b,k_o) = \int_o^{\theta_i} f_1(\theta,a,b,k_o)d\theta$$

and

$$G_{Ia}(\theta_i) = \int_{\theta_i}^{\infty} f_{1a}(\theta)d\theta \ .$$

For truncating the integral of $Im[I(a,b)]$, an analytical upper bound to $G_{Ia}(\theta_i)$ is sought for $\infty \geq k_o a \cosh\theta_i \geq 13$. We can easily show that:

$$f_{1a}(\theta) \leq \frac{2\left[\frac{1}{\sqrt{a}} + \frac{1}{\sqrt{b}}\right]^2}{\pi k_o^2 \cosh^2\theta}$$

or,

$$G_{Ia}(\theta_i) \leq \frac{2\left[\frac{1}{\sqrt{a}} + \frac{1}{\sqrt{b}}\right]^2}{\pi k_o^2} [1 - \tanh \theta_i]$$

$$= \text{upper}\,[G_{Ia}(\theta_i)] \qquad (3.12)$$

Since;

$$\int_o^x \frac{dt}{\cosh^2 t} = \tanh x$$

The functions $f_1(\theta,a,b,k_o)$, $f_2(\theta,n,a,b,x,k_o)$, and $f_3(\theta,n,a,b,k_o)$ are oscillatory due to the oscillatory behavior of the Bessel's functions appearing in each of them at large n.

The integral $G_I(\theta_i,a,b,k_o)$ is performed numerically by first numerically locating the zeros of the first derivative of $f_1(\theta,a,b,k_o)$ (from $\theta = 0$ to $\theta = \theta_i$), which correspond to the maxima and minima points of $f_1(\theta,a,b,k_o)$. As a second step we use a Gaussian quadrature scheme of numerical integration to integrate $f_1(\theta,a,b,k_o)$ in the intervals between consecutive maxima and minima points. This method allows good polynomial fit by reducing the curvature of integrand on the quarter cycles. If we define ζ to be a small positive number, at some angle $\theta_i = \theta_t$ (θ_t is the truncation value) we can assume truncation if:

$$\frac{|\text{upper}[G_{Ia}(\theta_t)]|}{|G_I(\theta_t,a,b,k_o)|} \leq \zeta$$

I assumed ζ to be 10^{-4}. Note that the integral value for $\theta > \theta_t$ is neglected and the value of the integral is good for the fourth decimal place. The truncation method discussed for Im[I(a,b)] integral is used for the integrals Im[$q_n(x)$] and Im[$J_{nn}(a,b)$] except that θ_i is chosen such as: $k_o a \cosh \theta_i \geq 13$ and ξ_n when $\xi_n > k_o$. To complete discussing integral evaluations, we here derive the upper bounds for the integrals Im[$q_n(x)$] and Im[$J_{nn}(a,b)$]. We can easily show that:

$$f_{2a}(\theta,n,a,b,x,k_o) \leq \frac{2\left[\frac{|J_o(\xi_n a)|}{\sqrt{b}} + \frac{|J_o(\xi_n b)|}{\sqrt{a}}\right]}{\pi\sqrt{x}\,(\xi_n^2 - k_o^2\cosh^2\theta)}$$

We also have (Gradshteyn and Ryzhik, 1965, p. 112):

$$\int_x \frac{d\theta}{A+B\cosh^2\theta} = \frac{1}{\sqrt{-A(A+B)}} \arctan\left[\sqrt{-(1+\frac{B}{A})}\,\coth x\right],$$

$$\frac{B}{A} < -1 \qquad (3.13)$$

$$= \frac{1}{\sqrt{A(A+B)}} \operatorname{arth}\left[\sqrt{1+\frac{B}{A}}\,\coth x\right],$$

$$-1 < \frac{B}{A} < 0 \text{ and } \cosh^2\theta < -\frac{A}{B} \qquad (3.14)$$

Where; $\operatorname{arth} z = \ln(\sqrt{1+z}/\sqrt{1-z})$.

$$\int_{\theta_i}^{\infty} f_{2a}(\theta,n,a,b,x,k_o) \leq \frac{2\left[\frac{|J_o(\xi_n a)|}{\sqrt{b}} + \frac{|J_o(\xi_n b)|}{\sqrt{a}}\right]}{\pi\sqrt{x}}$$

$$\cdot \int_{\theta_i}^{\infty} \frac{d\theta}{(\xi_n^2 - k_o^2 \cosh^2\theta)} \qquad (3.15)$$

The integral appearing at the right-hand side of (3.15) can be evaluated using (3.13) for $k_o > \xi_n$ and (3.14) for $\xi_n < k_o$. Hence, an upper bound for $\mathrm{Im}[q_n(x)]$ is obtained.

Looking for an upper bound for $\mathrm{Im}[J_{nn}(a,b)]$ we have:

$$f_{3a}(\theta,n,a,b,k_o) \leq \frac{2}{\pi}\left[\frac{|J_o(\xi_n a)|}{\sqrt{b}} + \frac{|J_o(\xi_n b)|}{\sqrt{a}}\right]^2 \frac{k_o^2 \cosh^2\theta}{(\xi_n^2 - k_o^2 \cosh^2\theta)^2} \qquad (3.16)$$

But:

$$\frac{k_o^2 \cosh^2\theta}{(\xi_n^2 - k_o^2 \cosh^2\theta)^2} = \frac{\xi_n^2}{(\xi_n^2 - k_o^2 \cosh^2\theta)^2} - \frac{1}{(\xi_n^2 - k_o^2 \cosh^2\theta)} .$$

Therefore:

$$\int_{\theta_i}^{\infty} \frac{k_o^2 \cosh^2\theta}{(\xi_n^2 - k_o^2 \cosh^2\theta)^2} d\theta = \xi_n^2 \int_{\theta_i}^{\infty} \frac{d\theta}{(\xi_n^2 - k_o^2 \cosh^2\theta)^2} - \int_{\theta_i}^{\infty} \frac{d\theta}{(\xi_n^2 - k_o^2 \cosh^2\theta)} \tag{3.17}$$

From Gradshteyn and Ryzhik (1965, p. 113), we have:

$$\int \frac{dx}{(A+B\cosh^2 x)^2} = \frac{1}{2A(A+B)} \left[\frac{-B \sinh x \cosh x}{A+B\cosh^2 x} + (2A+B) \int \frac{dx}{A+B\cosh^2 x} \right] \tag{3.18}$$

Using equations (3.18), (3.16), (3.14), or (3.15), an upper bound for the imaginary part of the integral $J_{nn}(a,b)$ is achieved.

Note that in the case of $k_o > \xi_n$, the singularity of $\alpha = \xi_n$ does not appear in the imaginary parts of integrals $q_n(x)$, $J_{nn}(a,b)$, but does appear in the real parts. This is to be seen in the plots given in Chapter 5.

CHAPTER 4

ANALYSIS OF THE EDGE SINGULARITY

The edge condition states that the energy density must be integrable over any finite domain. If the dielectric of region 1 is air, the edge condition gives that the radial component of the electric field at the aperture must be singular at $\rho = a$ and $\rho = b$ (Meixner, 1954), and the order of these singularities is 1/3. In this chapter we will use this edge condition to estimate the relative behavior of the TM mode amplitudes in the guide region when n is large ($n > N$). From equation (2.9) we have:

$$E\rho_1(\rho,o) = \frac{(1+\Gamma_o)T_o}{\rho} + \sum_{n=1}^{\infty} \frac{Y_n}{\xi_n} T_n Q_o'(\xi_n\rho)$$

Where; $Q_o'(\xi_n\rho) = Y_o(\xi_n a)J_1(\xi_n\rho) - J_o(\xi_n a)Y_1(\xi_n\rho)$

If we let: $t_n = \frac{T_n Y_n}{\pi \xi_n^2 T_o}$ and $e\rho_1(\rho,o) = E\rho_1(\rho,o)/T_o$, we get:

$$e\rho_1(\rho,o) = \frac{(1+\Gamma_o)}{\rho} + \sum_{n=1}^{N} t_n \pi \xi_n Q_o'(\xi_n\rho)$$

$$+ \sum_{m=N+1}^{\infty} t_m \pi \xi_m Q_o'(\xi_n\rho) \qquad (4.1)$$

The summation in the far right-hand side of equation (4.1) represents the higher order TM modes contribution to the

aperture field. This contribution is expected to count for the singularities at $\rho = a$ and $\rho = b$ (this will be shown in the next chapter). A good way to look at it, is that the summation over m in equation (4.1) represents high frequency terms summation whose effect is more to build any discontinuities in the aperture field.

From Meixner (1954), we can let:

$$\sum_{m=N+1}^{\infty} \pi \xi_m t_m Q_o'(\xi_n \rho) \tilde{=} \frac{D_a}{(b-\rho)^{1/3}} + \frac{D_b}{(\rho-a)^{1/3}} . \qquad (4.2)$$

Where D_a and D_b are any arbitrary constants. If we integrate both sides of equation (4.2) with respect to ρ from $\rho = a$ to $\rho = b$ we get:

$$D_a + D_b = 0$$

Now multiply both sides of equation (4.2) by $\rho Q_o'(\xi_m' \rho)$ and integrate from $\rho = a$ to $\rho = b$, hence:

$$\sum_{m=N+1}^{\infty} \pi \xi_m t_m \int_a^b Q_o'(\xi_m \rho) Q_o'(\xi_m' \rho) \rho d\rho \tilde{=} D_a \left[\int_a^b \frac{\rho Q_o'(\xi_m' \rho)}{(b-\rho)^{1/3}} d\rho \right.$$

$$\left. - \int_a^b \frac{Q_o'(\xi_m' \rho)}{(\rho-a)^{1/3}} d\rho \right] \qquad (4.3)$$

From Chapter 2, we derived the following result:

$$\int_a^b Q_o'(\xi_m \rho) Q_o'(\xi_m' \rho) \rho d\rho = - \delta_{mm'} \frac{2 Z_m'(a,b)}{(\pi \xi_{m'})^2} \qquad (4.4)$$

Where: $\delta_{mm'} = 0 \qquad m \neq m'$

$= 1 \qquad m = m'$

$$Z_{m'}(a,b) = 1 - \left[\frac{J_o(\xi_{m'}a)}{J_o(\xi_{m'}b)} \right]^2 .$$

From equations (4.3) and (4.4) we can write that:

$$\frac{2Z_m(a,b)}{\pi\xi_m} \cong D_a\left[\int_a^b \frac{\rho Q_o'(\xi_m\rho)}{(\rho-a)^{1/3}}\, d\rho - \int_a^b \frac{\rho Q_o'(\xi_m\rho)}{(b-\rho)^{1/3}}\, d\rho \right] \tag{4.5}$$

Since m in equation (4.5) is large, an asymptotic behavior of ξ_m as m gets large is to be derived. For large argument z we have:

$$J_n(z) \cong \frac{2}{\pi z} \cos\left(z - \frac{n\pi}{2} - \pi/4\right)$$

$$Y_n(z) \cong \frac{2}{\pi z} \sin\left(z - \frac{n\pi}{2} - \pi/4\right)$$

Using the two previous approximations, the eigen values are then defined by:

$$\xi_m \cong \frac{m\pi}{(b-a)}$$

and

$$\frac{J_o(\xi_m a)}{J_o(\xi_m b)} \cong (-1)^m \frac{b}{a}$$

$$Z_m(a,b) \cong \frac{(a-b)}{a} .$$

For large m, we can easily show that:

$$Q_o'(\xi_m\rho) \cong \frac{2\cos[\xi_m(\rho-a)]}{\pi\xi_m\sqrt{a\rho}}$$

Using the previous discussion, equation (4.5) becomes:

$$\frac{(b-a)}{\sqrt{a}\,D_a}\,t_m \cong R_m[e^{-i\xi_m a}\{\int_a^b \frac{\sqrt{\rho}\,e^{i\xi_m\rho}}{(b-\rho)^{1/3}}\,d\rho - \int_a^b \frac{\sqrt{\rho}\,e^{i\xi_m\rho}}{(\rho-a)^{1/3}}\,d\rho\}] \tag{4.6}$$

$$\int_a^b \frac{\sqrt{\rho}\,e^{i\xi_m\rho}}{(b-\rho)^{1/3}}\,d\rho = \int_a^b \frac{(\sqrt{\rho}-\sqrt{a})e^{i\xi_m\rho}}{(b-\rho)^{1/3}}\,d\rho + \sqrt{a}\int_a^b \frac{e^{i\xi_m\rho}}{(b-\rho)^{1/3}}\,d\rho$$

From Copson (1965, p. 24), we have:

$$\int_\alpha^\beta e^{i\nu x}(\beta-x)^{\mu-1}\phi(x)\,dx = \sum_{n=o}^{M-1} \frac{\Gamma(n+\mu)}{n!\,\nu^{n+\mu}}\,e^{i\nu\beta - \frac{\mu\pi i}{2} + \frac{n\pi i}{2}}\,\phi^n(\beta) + O(\nu^{-M}) \tag{4.7}$$

$\phi(x)$ is M times continuously differentiable in $\alpha \le x \le \beta$, $\phi(x)$ and its first M-1 derivatives vanish when $x = \alpha$, $0 < \mu < 1$ and $\nu \to \infty$. Note that:

$$\phi^n(\beta) = \frac{d^n}{dx^n}\,\phi(x)\Big|_{x=\beta}$$

If we take the first term in the summation appearing in equation (4.7) as an approximation, we have:

$$\int_a^b \frac{(\sqrt{\rho} - \sqrt{a})e^{i\xi_m\rho}}{(b-\rho)^{1/3}}\,d\rho = \frac{\Gamma(2/3)}{\xi_m^{2/3}}\, e^{-\pi i/3}\, e^{i\xi_m b} \cdot$$

$$\cdot\, [\sqrt{b} - \sqrt{a}] + O(1/\xi_m) \qquad (4.8)$$

Also, from Copson (1965, p. 23), we have:

$$\int_\alpha^\beta e^{i\nu x}(x-\alpha)^{\lambda-1}\phi(x)\,dx = \sum_{n=o}^{M-1} \frac{\Gamma(n+\lambda)}{n!\nu^{n+\lambda}}\, e^{i\nu\alpha + \frac{\pi i\lambda}{2} + \frac{n\pi i}{2}} \cdot$$

$$\cdot\, \phi^n(\alpha) + O(\nu^{-M})$$

$\phi(x)$ again is M times continuously differentiable in $\alpha \leq x \leq \beta$, $\phi(x)$ and its first M-1 derivatives vanish at $x = \beta$, $0 < \lambda < 1$ and $\nu \to \infty$. Therefore:

$$\int_a^b \frac{(\sqrt{\rho} - \sqrt{b})e^{i\xi_m\rho}}{(\rho-a)^{1/3}}\,d\rho = \frac{\Gamma(2/3)}{\xi_m^{2/3}}\, e^{\pi i/3}\, e^{i\xi_m a} \cdot$$

$$\cdot\, (\sqrt{a} - \sqrt{b}) + O(1/\xi_m)$$

The integrals left to evaluate in equation (4.6) are:

$$w_1(m,a,b) = \int_a^b \frac{e^{i\xi_m\rho}}{(b-\rho)^{1/3}}\,d\rho$$

$$w_2(m,a,b) = \int_a^b \frac{e^{i\xi_m\rho}}{(\rho-a)^{1/3}}\,d\rho$$

If we make the changes of variables $\rho = b - z/\varepsilon_m$ and $\rho = a + z/\varepsilon_m$ in $w_1(m,a,b)$ and $w_2(m,a,b)$ respectively we get

$$w_1(m,a,b) = e^{i\xi_m b}\, \xi_m^{-2/3} \int_0^{m\pi} z^{-1/3}\, e^{-iz}\, dz$$

$$w_2(m,a,b) = e^{i\xi_m a}\, \xi_m^{-2/3} \int_0^{m\pi} z^{-1/3}\, e^{iz}\, dz$$

From the previous discussion, equation (4.6) takes the form:

$$\frac{(b-a)}{\sqrt{a}\, D_a}\, t_m = \frac{\Gamma(2/3)(\sqrt{b} - \sqrt{a})}{2\xi_m^{2/3}} [1+(-1)^m]$$

$$-\left[\frac{\sqrt{b} - (-1)^m\sqrt{a}}{\xi_m^{2/3}}\right] \int_0^{m\pi} \frac{\cos z\, dz}{z^{1/3}} \qquad (4.9)$$

From Gradshteyn and Ryzhik (1965, p. 421), we have:

$$\int_c^{\infty} x^{\mu-1} \cos x\, dx = \frac{1}{2}\left[e^{-\frac{\pi\mu i}{2}}\, \Gamma(\mu, ic)\right.$$

$$\left. + e^{\frac{\pi\mu i}{2}}\, \Gamma(\mu, -ic)\right], \quad \mathrm{Re}\,\mu < 1 \qquad (4.10)$$

$$\int_0^{\infty} x^{\mu-1} \cos x\, dx = \Gamma(\mu) \cos\left(\frac{\mu\pi}{2}\right), \quad 0 < \mathrm{Re}\,\mu < 1$$

(4.11)

From equations (4.10) and (4.11), we find that:

$$\int_0^{m\pi} \frac{\cos z}{z^{1/3}}\, dz = \frac{\Gamma(2/3)}{2} - \frac{1}{2}\left[e^{-\pi i/3}\Gamma(2/3, im\pi)\right.$$

$$\left. + e^{i\pi/3}\Gamma(2/3, -im\pi)\right] \qquad (4.12)$$

For $m \to \infty$ we can neglect the second expression to the right-hand side of equation (4.12) involving the incomplete gamma functions, hence:

$$\int_0^{m\pi} \frac{\cos z}{z^{1/3}}\, dz \cong \frac{\Gamma(2/3)}{2} \qquad (4.13)$$

From equation (4.9) and (4.13), we can write:

$$t_m \cong \frac{\sqrt{a}\, D_a \Gamma(2/3)}{2(b-a)\xi_m^{2/3}}\left[(\sqrt{b} - \sqrt{a})(1+(-1)^m)\right.$$

$$\left. - (\sqrt{b} - (-1)^m \sqrt{a})\right] \qquad (4.14)$$

Note that from equation (4.14), we can find t_{m+2} once we know what t_m is or:

$$t_{m+2} \cong \left(\frac{m}{m+2}\right)^{2/3} t_m$$

The process of evaluating the higher order t_m from the previously calculated by solving the matrix equation becomes essential when $(b-a)/\lambda_o \geq 0.5$ where bigger matrix should be solved.

Another feature of this analysis is that it gives a correction to the error due to truncating the infinite set of linear equations into a finite one. This is done as follows. The original matrix equation (2.30) is:

$$\sum_{m=1}^{\infty} L_{nm} t_m = f_n(a,b)$$

or

$$\sum_{m=1}^{N} L_{nm} t_m = f_n'(a,b)$$

where

$$f_n'(a,b) = f_n(a,b) - \sum_{m=N+1}^{\infty} L_{nm} t_m$$

Even though I did not use the edge conditions in all my calculations, I think that its analysis is a part of solving this problem especially when the aperture starts to be comparable to a wave length.

CHAPTER 5

THE FIELD PATTERN AND NUMERICAL RESULTS

An important feature in the design of an antenna is the far field pattern. This is done in this chapter before looking at the numerical results. From the uniqueness concept, the tangential component of only the magnetic field or the electric field at the aperture is needed to determine the fields for $z > 0$. Due to the fact that the tangential component of the electric field $E_{\rho_1}(\rho,o)$ vanishes everywhere except at the aperture, an equivalent magnetic current, $\bar{M}_s$, is utilized.

From Figure 3, the far field pattern can be evaluated using the equivalence principle and image theory. Now let,

$$E_{\rho_1}(\rho',o) = E_a(\rho')$$

$$\bar{M}_s = -\hat{u}_\phi E_a(\rho') \qquad b \geq \rho' \geq a$$

$$= 0 \qquad \text{elsewhere}$$

From Figure 3(c), the electric vector potential at any point $P(r,\phi_o,\theta)$ in region 2 is:

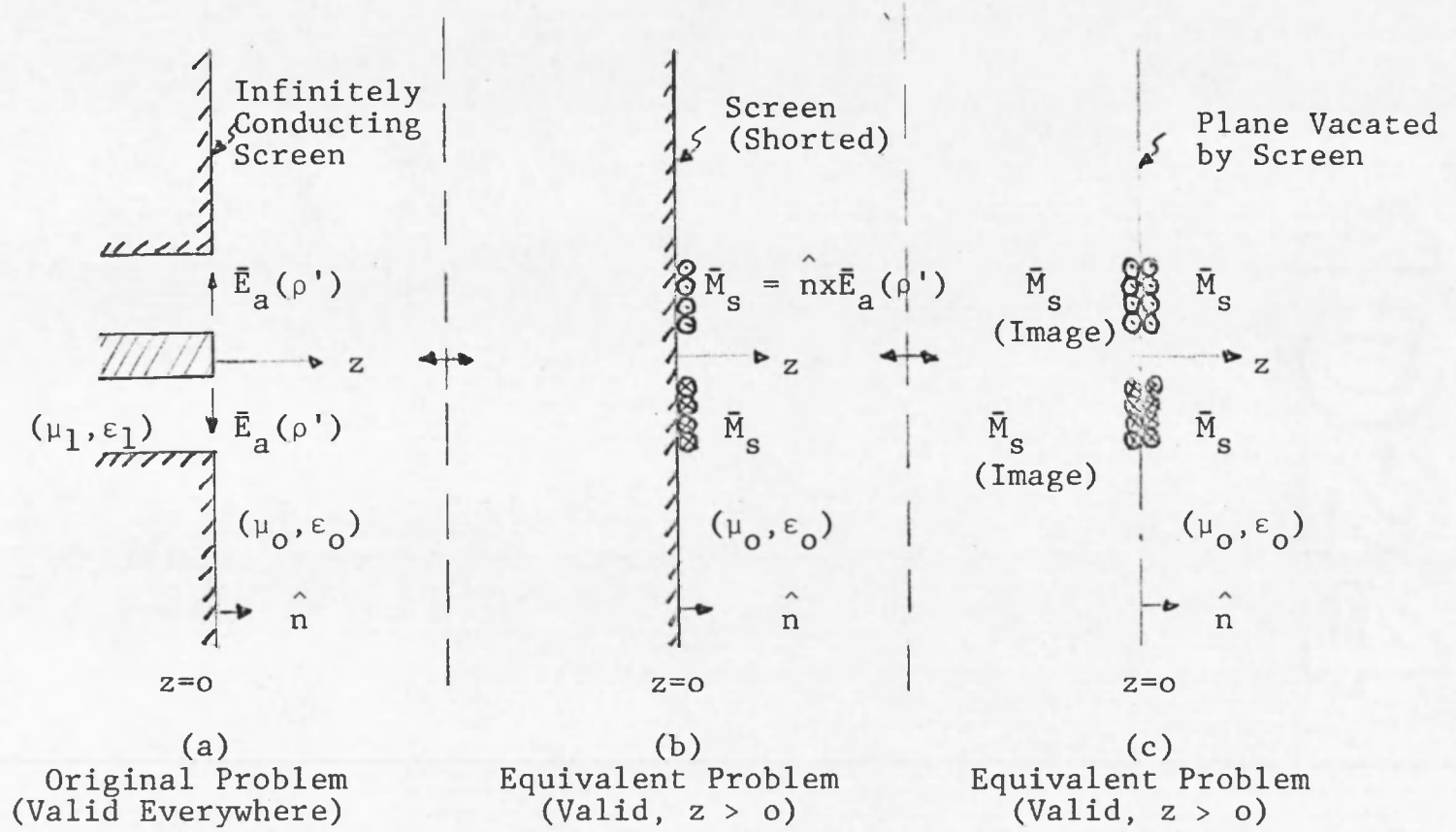

Figure 3. Right half-space equivalent problem.

$$\overline{F} = \frac{1}{4\pi} \iint_{\text{aperture}} 2\overline{M}_s \frac{e^{-ik_o R}}{R} \, ds'$$

$$= -\frac{1}{2\pi} \int_{\rho'=a}^{b} \int_{\phi'=\pi}^{\pi} E_a(\rho') \hat{u}_{\phi'} \frac{e^{-ik_o R}}{R} \, \rho' d\phi' d\rho' \tag{5.1}$$

Where $R = |\overline{r} - \overline{\rho}'|$. In the far field, from Figure 4 we have:

$$R^2 = \gamma^2 + z^2$$

$$= r^2 + \rho'^2 - 2r\rho' \sin\theta \cos(\phi' - \phi_o)$$

If $r >> \rho'$ we get:

$$R \tilde{=} r - \rho' \sin\theta \cos(\phi' - \phi_o)$$

From Figure 5, we also have:

$$\hat{u}_{\phi'} = \hat{u}_\phi \cos(\phi' - \phi_o) - \hat{u}_r \sin(\phi' - \phi_o)$$

Upon setting $\phi_o = 0$ equation (5.1) takes the form:

$$\overline{F} = \frac{-e^{-ik_o r}}{2\pi r} \int_{\rho'=a}^{b} \rho' d\rho' \int_{\phi'=-\pi}^{\pi} E_a(\rho') [\hat{u}_\phi \cos\phi' - \hat{u}_r \sin\phi'] e^{ik_o \rho' \sin\theta \cos\phi'} \, d\phi$$

Note that the radial part of $\overline{F}$ vanishes, therefore:

$$F_\phi = \frac{-e^{-ik_o r}}{2\pi r} \int_{\rho'=a}^{b} E_a(\rho') \rho' d\rho' \cdot \cdot \int_{\phi'=-\pi}^{\pi} \cos\phi' e^{ik_o \rho' \sin\theta \cos\phi'} \, d\phi'$$

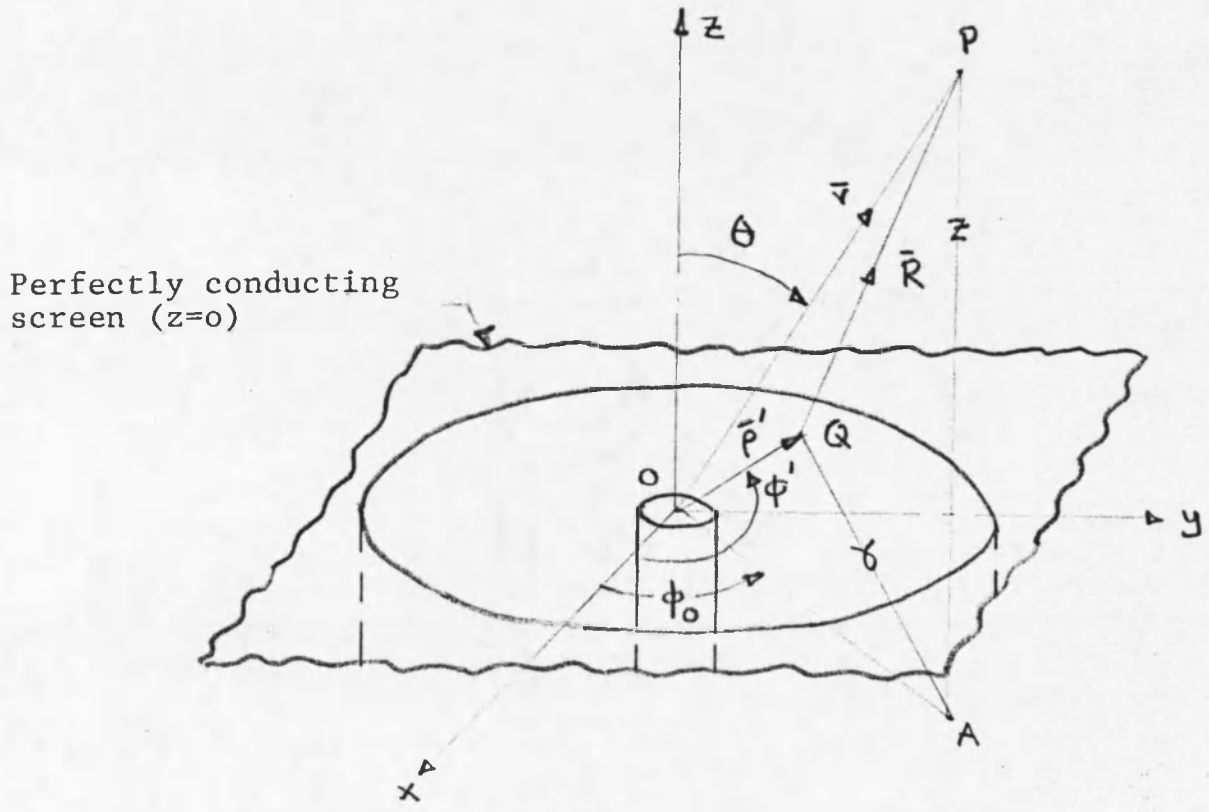

Figure 4. The coordinate systems of region 2 and the source aperture.

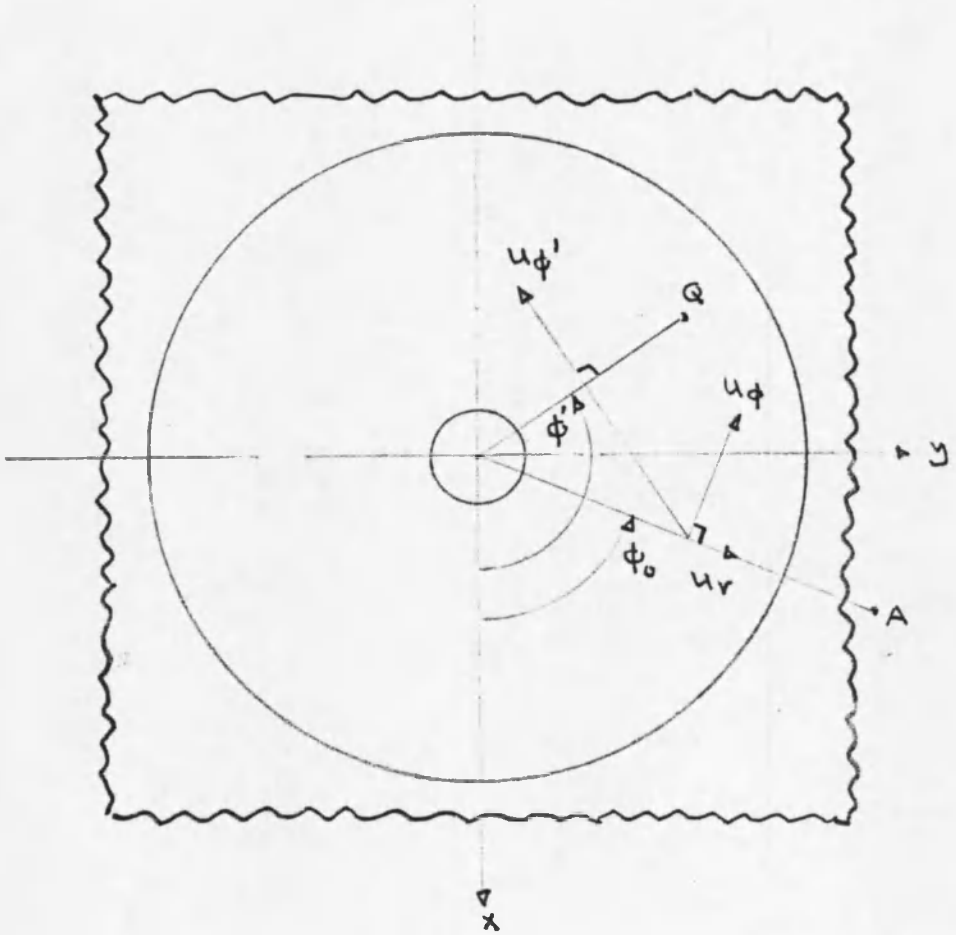

Figure 5. A top view of the aperture.

We can easily show that:

$$\int_{\phi'=-\pi}^{\pi} \cos\phi' e^{ik_o\rho' \sin\theta \cos\phi'} d\phi'$$

$$= 2i\pi J_1(k_o\rho \sin\theta)$$

Hence;

$$\overline{F} = \frac{-ie^{-ik_o r}}{r} \int_a^b E_a(\rho') J_1(k_o\rho' \sin\theta)\rho' d\rho' \cdot \hat{\mu}_\phi$$

In the far field both the magnetic and electric radial components vanish and the magnetic field is determined explicitly by:

$$\overline{H} = -i\omega\varepsilon_o \overline{F}_t$$

Where $\overline{F}_t$ is the transverse component of $\overline{F}$. Therefore:

$$H_\phi(r,o,\theta) = -\frac{\omega\varepsilon_o e^{-ik_o r}}{r} \int_{\rho'=a}^{b} E_a(\rho') J_1(k_o\rho' \sin\theta)\rho' d\rho' \qquad (5.2)$$

In far field, we also have:

$$\hat{u}_\rho x\overline{H} = -\frac{\overline{E}}{\eta_o}$$

where $\eta_o = \sqrt{\mu_o/\varepsilon_o}$, therefore:

$$E_\theta = -\frac{k_o e^{-ik_o r}}{r} \int_{\rho'=a}^{b} E_a(\rho') J_1(k_o\rho' \sin\theta)\rho' d\rho' \qquad (5.3)$$

From equations (5.2) and (5.3), we can write the field pattern $G(\theta)$ to be:

$$G(\theta) = g \int_{\rho'=a}^{b} E_a(\rho') J_1(k_o \rho' \sin\theta) \rho' d\rho' \qquad (5.4)$$

Where g is an arbitrary constant to normalize the maximum value of $G(\theta)$ to be unity. From equation (4.1) in the previous chapter, we have:

$$E_a(\rho') = \frac{(1+\Gamma_o)}{\rho'} + \sum_{n=1}^{\infty} \pi \xi_n t_n Q_o'(\xi_n \rho') \qquad (5.5)$$

$$Q_o'(\xi_n \rho') = Y_o(\xi_n a) J_1(\xi_n \rho') - J_o(\xi_n a) Y_1(\xi_n \rho')$$

We also showed in Chapter 2 that:

$$\int_a^b Q_o'(\xi_n \rho) J_1(\alpha' \rho) \rho d\rho = \frac{2\alpha' R_n(\alpha')}{\pi \xi_n (\xi_n^2 - \alpha'^2)} \qquad (5.6)$$

$$R_n(\alpha') = \frac{Q_n(\alpha')}{J_o(\xi_n b)}$$

$$Q_n(\alpha') = J_o(\xi_n a) J_o(\alpha' b) - J_o(\xi_n b) J_o(\alpha' a)$$

From equations (5.4), (5.5), and (5.6) we have:

$$G(\theta) = g\Bigg[\frac{(1+\Gamma_o)\,[J_o(k_o a \sin\theta) - J_o(k_o b \sin\theta)]}{k_o \sin\theta} + \sum_{n=1}^{\infty} \frac{2k_o \sin\theta\, Q_n(k_o \sin\theta)}{J_o(\xi_n b)(\xi_n^2 - k_o^2 \sin^2\theta)}\, t_n \Bigg] \qquad (5.7)$$

for constant values of a = 0.05 and b = 0.1 meter, two far field patterns were plotted in Figure 6. The first plot

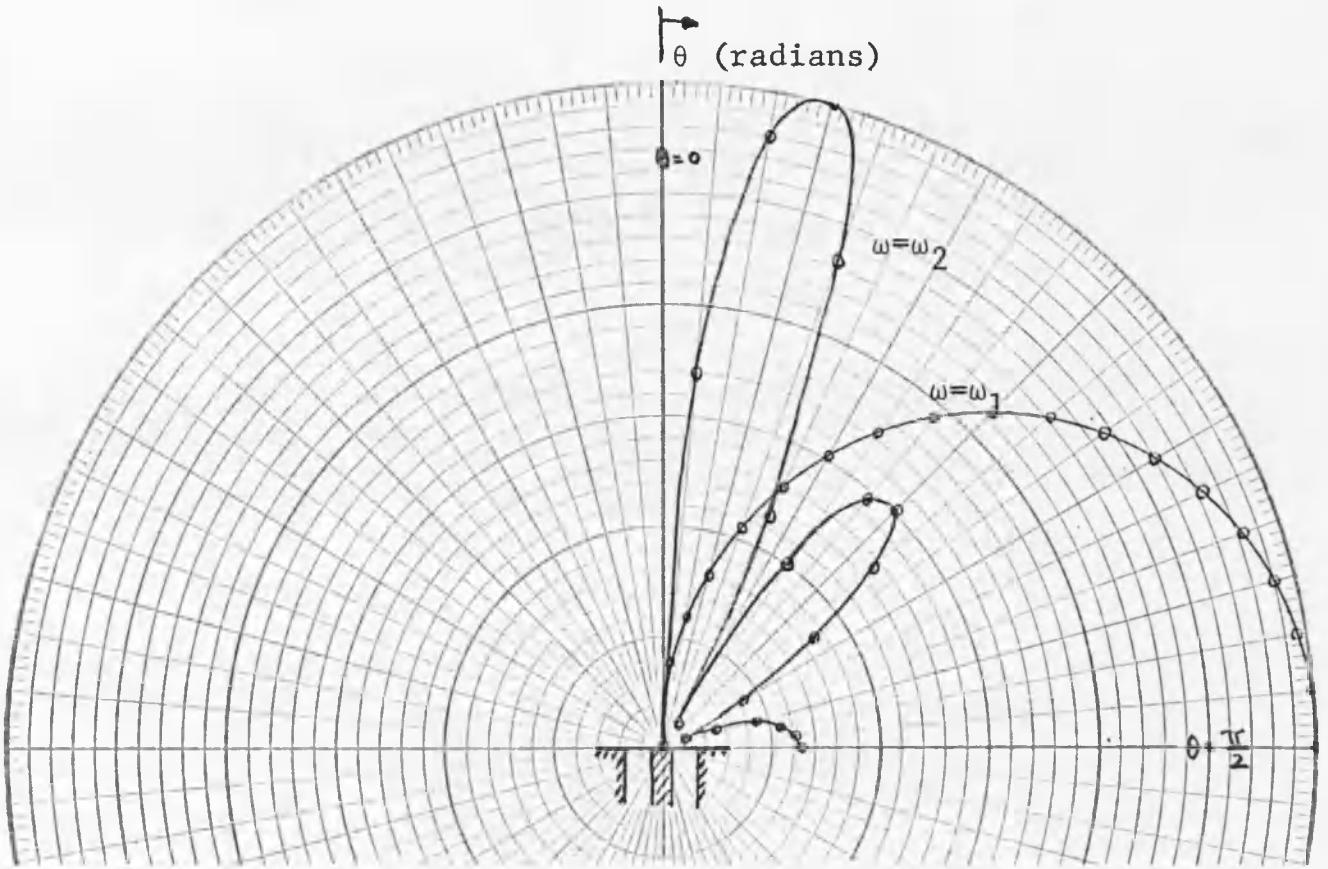

Figure 6. Two far field patterns.

corresponds to $\omega = \omega_1 = 2.5 \times 10^8$ rad/sec or $(b-a)/\lambda_o = 0.67 \times 10^{-2}$ knowing that $\xi_1 = 62.46$ the max occurred at $\theta = \pi/2$. For $\omega = \omega_2 = 2.79 \times 10^{10}$ rad/sec or $(b-a)/\lambda_o = 0.74$, two lobes resulted in the pattern. The first one at $\theta \tilde{=} 0.26$ rad is caused by the first term in the right-hand side of equation (5.7), and the second lobe is at $\theta \tilde{=} 0.74$ rad, resulting from $\xi_1 = k_o \sin\theta$ which is due to the second term in equation (5.7).

My major contribution to the problem is solving the integrals discussed in Chapter 3. Plots of the real and imaginary part integrands are plotted in Figures 7 to 15. It is clear in these plots that integrals as functions of n have their largest contribution in the vicinity of $\alpha = \xi_n$. The two frequencies considered are ω_1 and ω_2 mentioned above.

Another characteristic of the antenna to look at is its input admittance, since this is essential when the antenna is simply a circular aperture radiator or a feeding coaxial to another antenna. This is done by considering the effect of 30 TM (to z) modes on the TEM input admittance derived earlier using variational techniques by Marcuvitz (1951, pp. 214-215). Figures 16 and 17 show plots of the normalized input conductance G/Y_o and the normalized input susceptance B/Y_o, where Y_o represents the characteristic admittance of the coaxial guide:

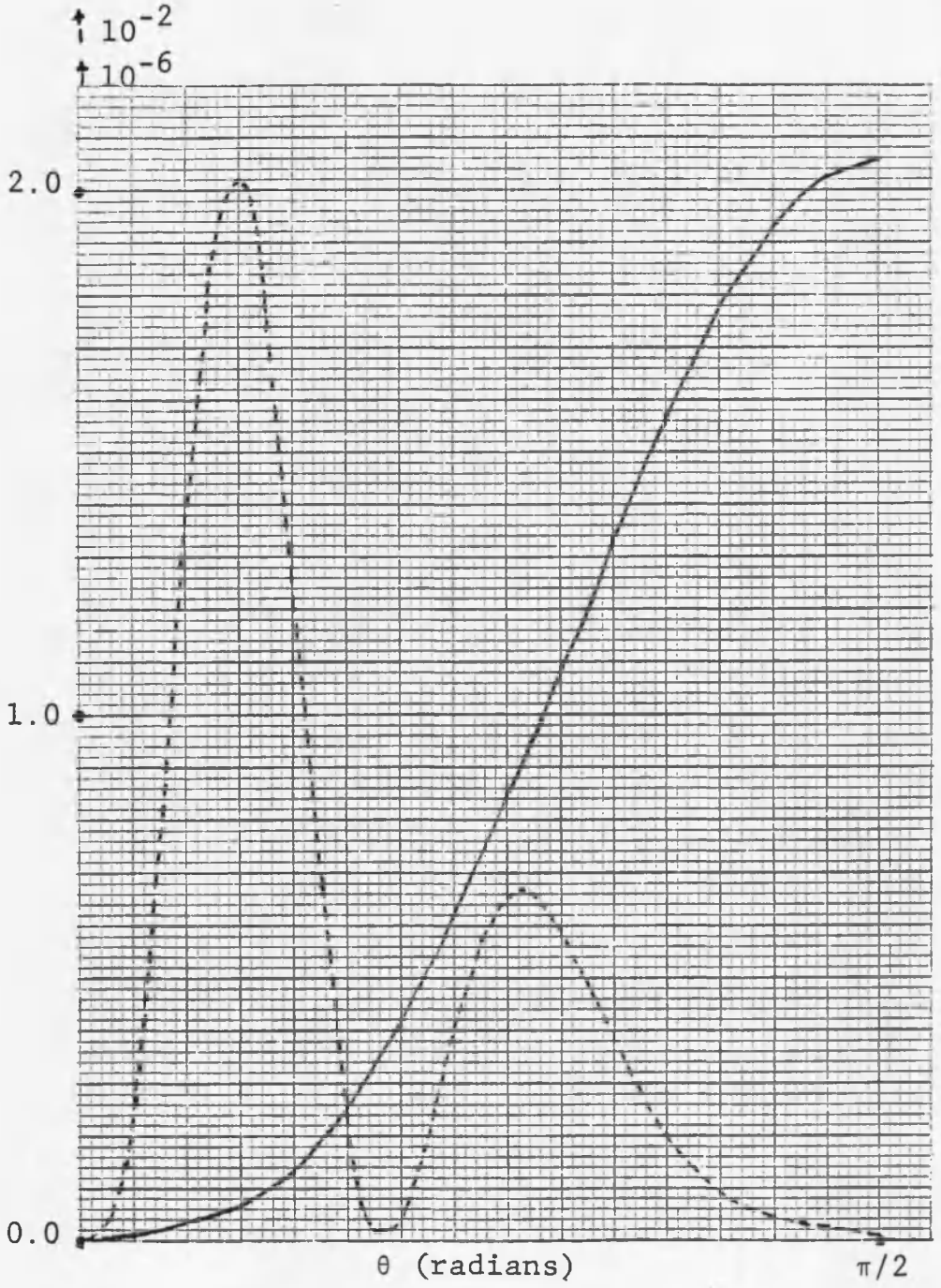

Figure 7. Graphs of the integrand of Re[I(0.05,0.1)], for $\omega = \omega_1$ (———) and $\omega = \omega_2$ (-----).

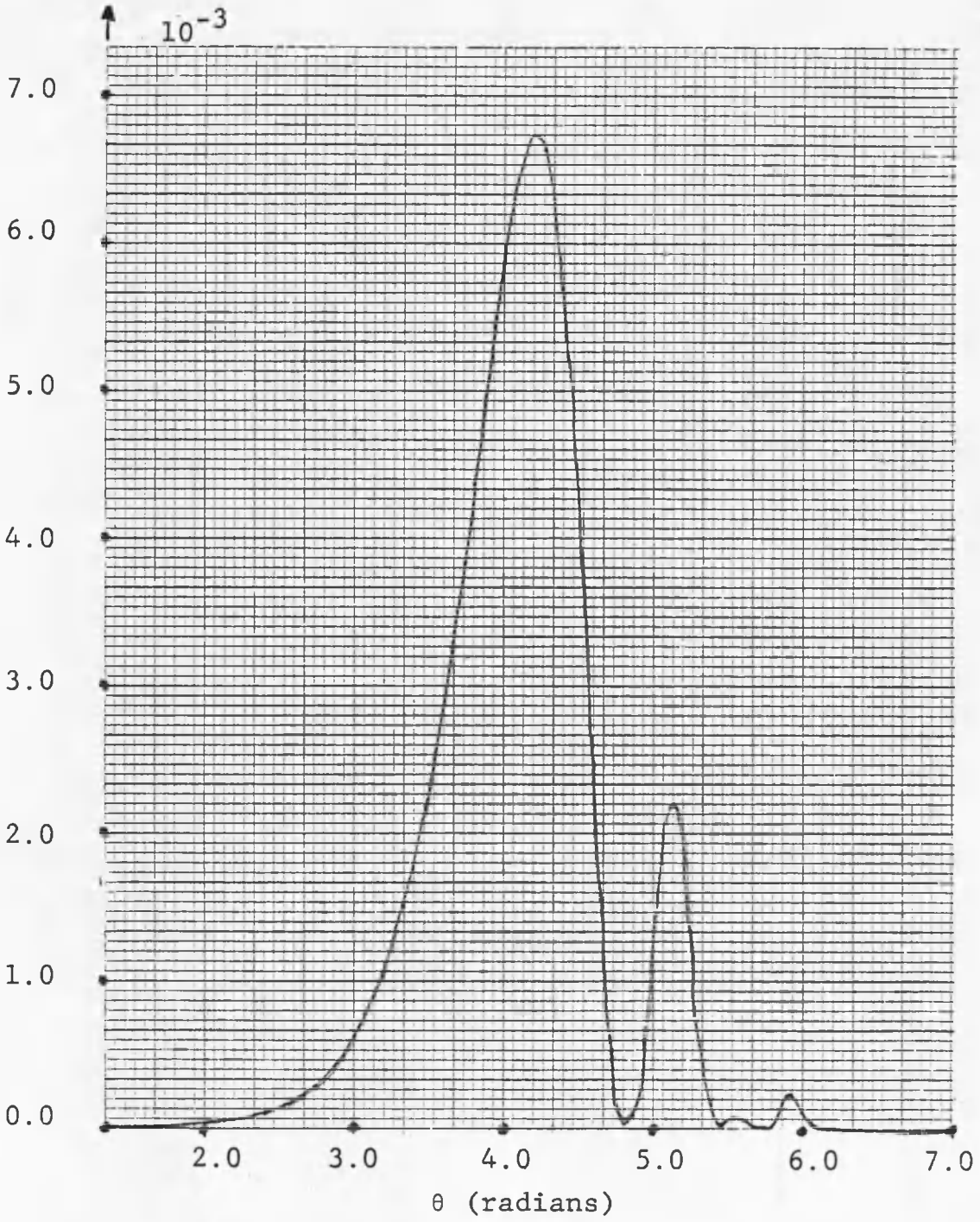

Figure 8. A graph of the integrand of Im[I(0.05,0.1)], for $\omega = \omega_1$.

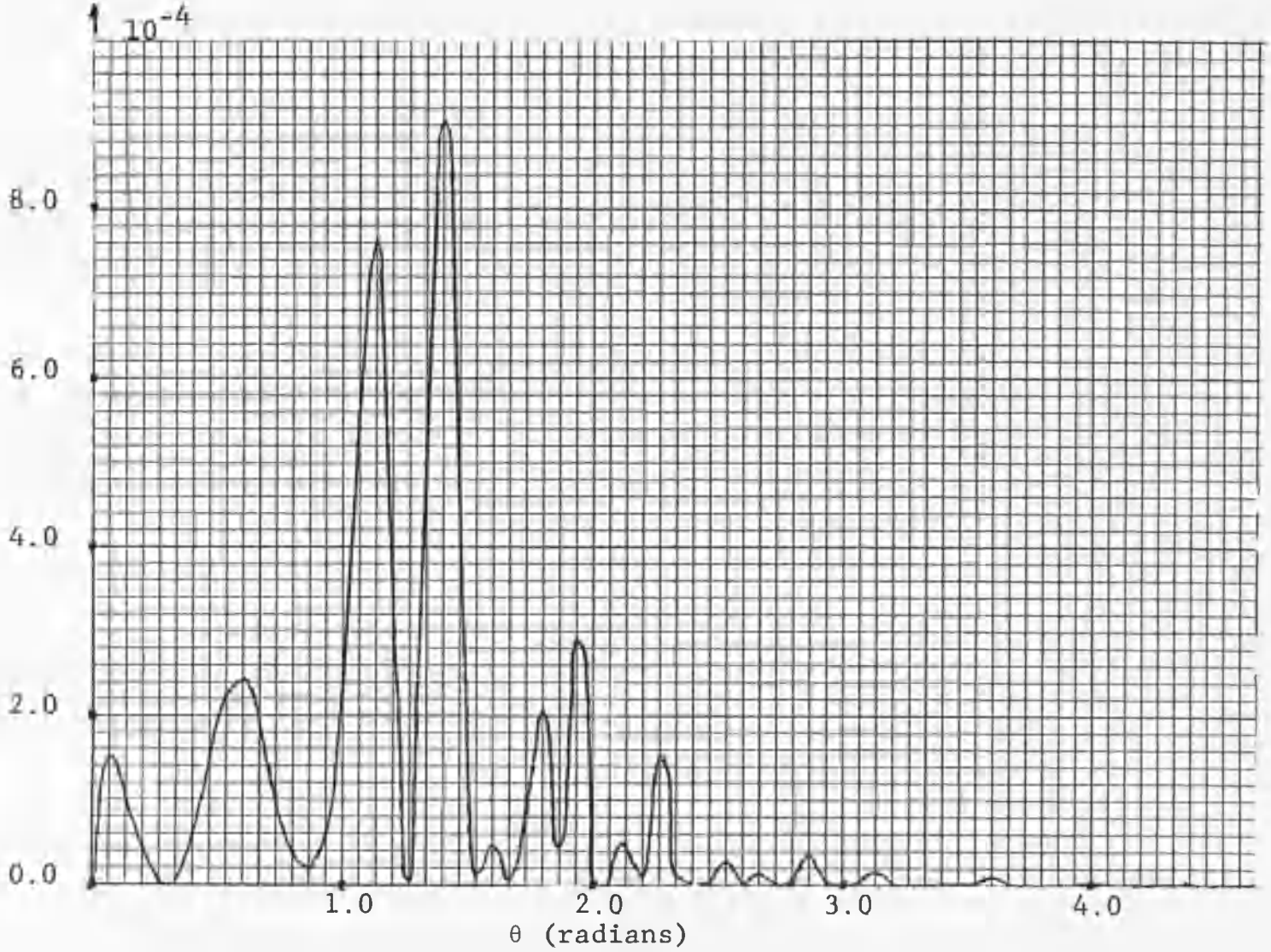

Figure 9. A graph of the integrand of Im[I(0.05,0.1)], for $\omega = \omega_2$.

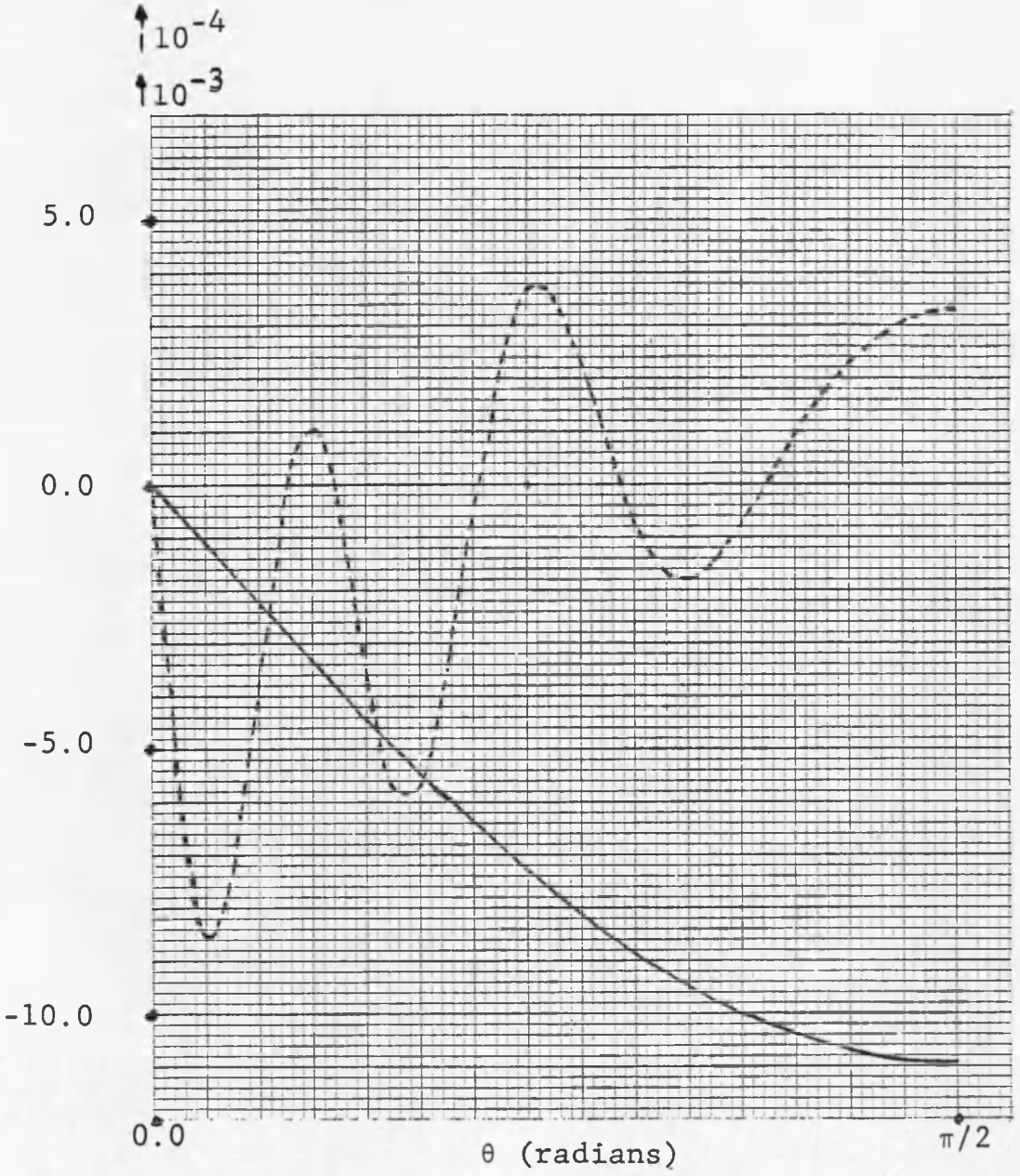

Figure 10. Graphs of the integrands of $\mathrm{Re}[q_1(0.1)]$, for $\omega = \omega_1$ (———) and $\omega = \omega_2$ (-----).

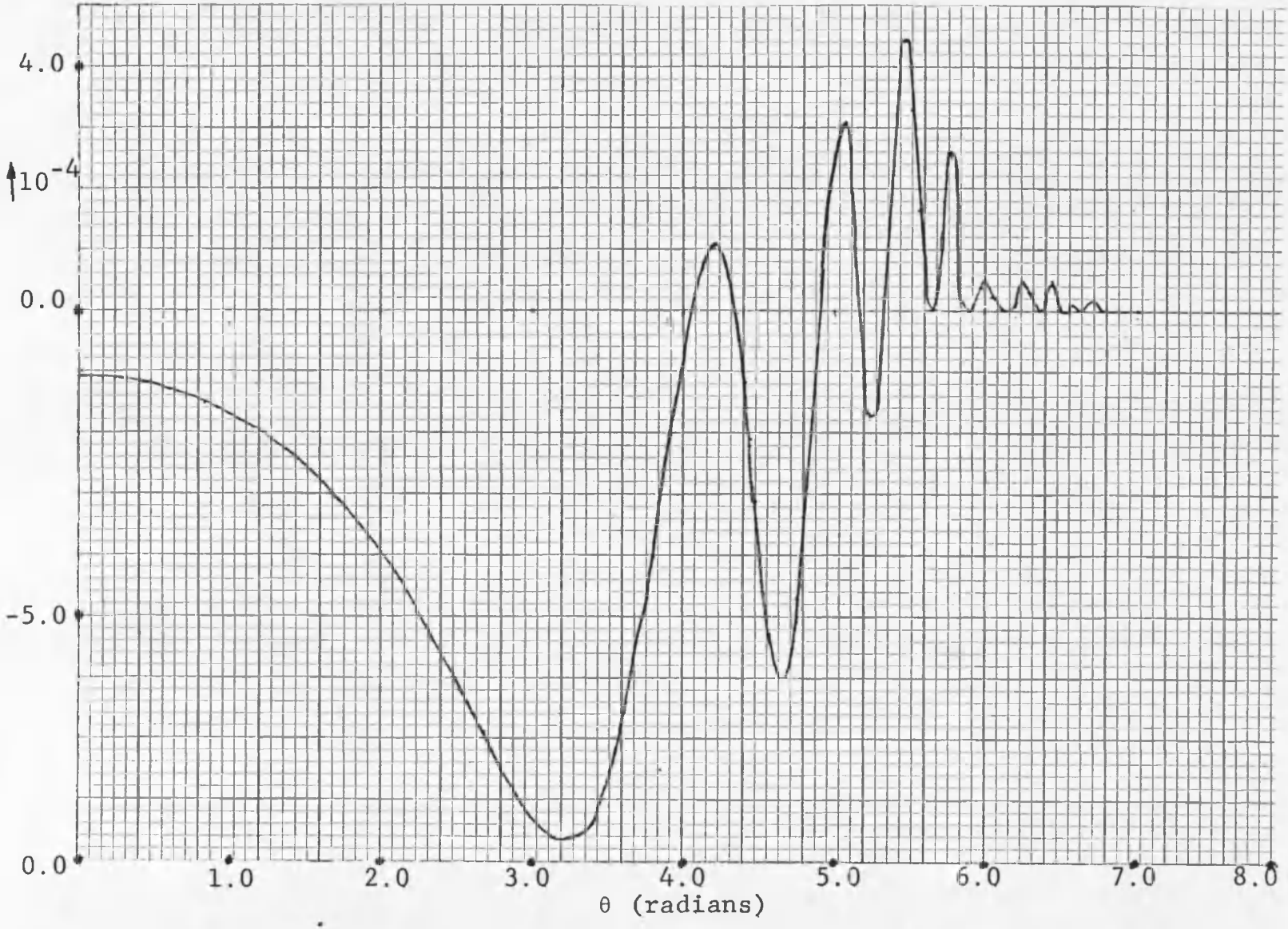

Figure 11. A graph of the integrand of $\mathrm{Im}[q_1(0.1)]$, for $\omega = \omega_1$.

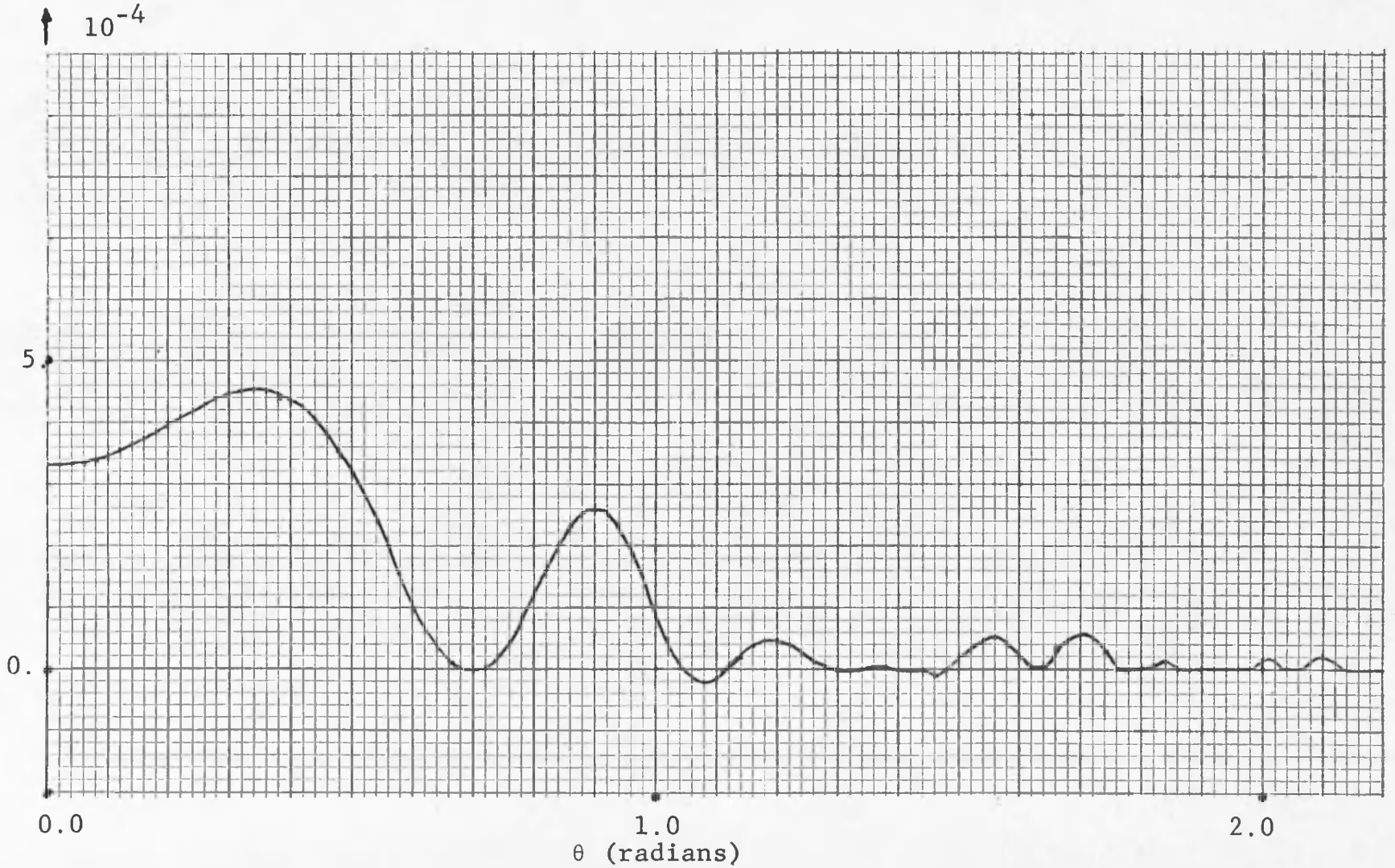

Figure 12. A graph of the integrand of $\mathrm{Im}[q_1(0.1)]$, for $\omega = \omega_2$.

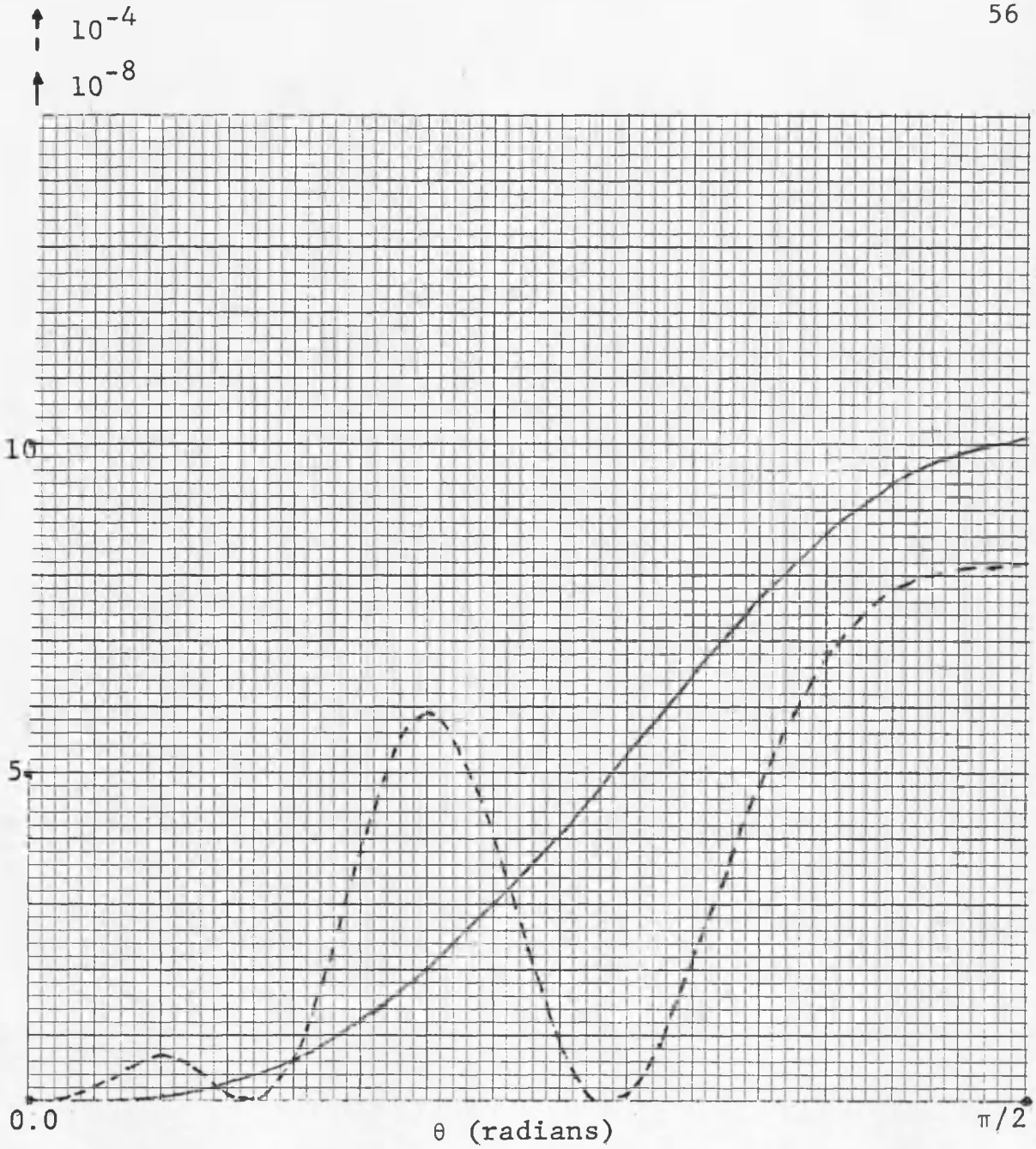

Figure 13. Graphs of the integrand of $\mathrm{Re}[J_{11}(0.05,0.1)]$, for $\omega = \omega_1$ (———) and $\omega = \omega_2$ (-----).

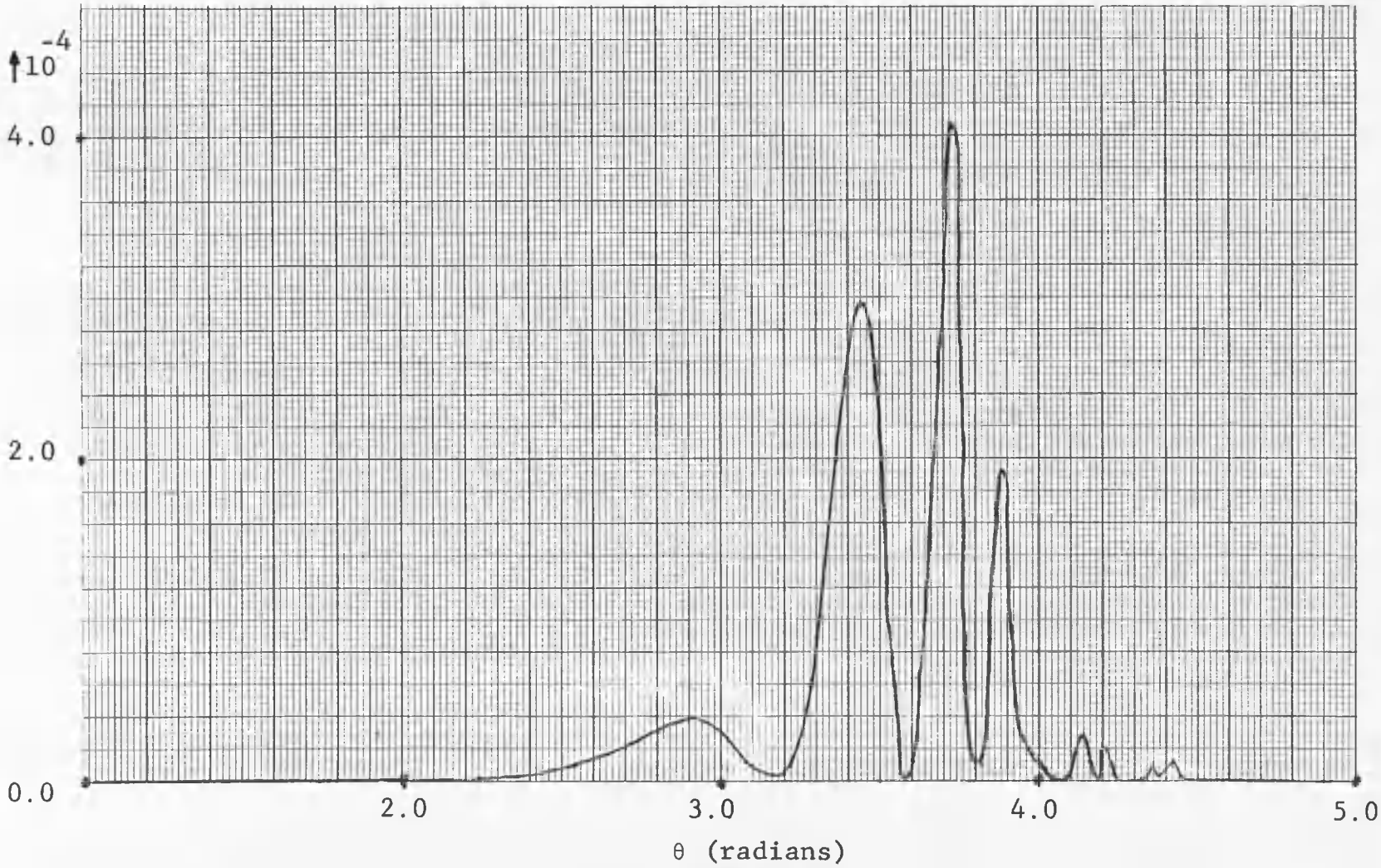

Figure 14. A graph of the integrand of $\mathrm{Im}[J_{11}(0.05,0.1)]$, for $\omega = \omega_1$.

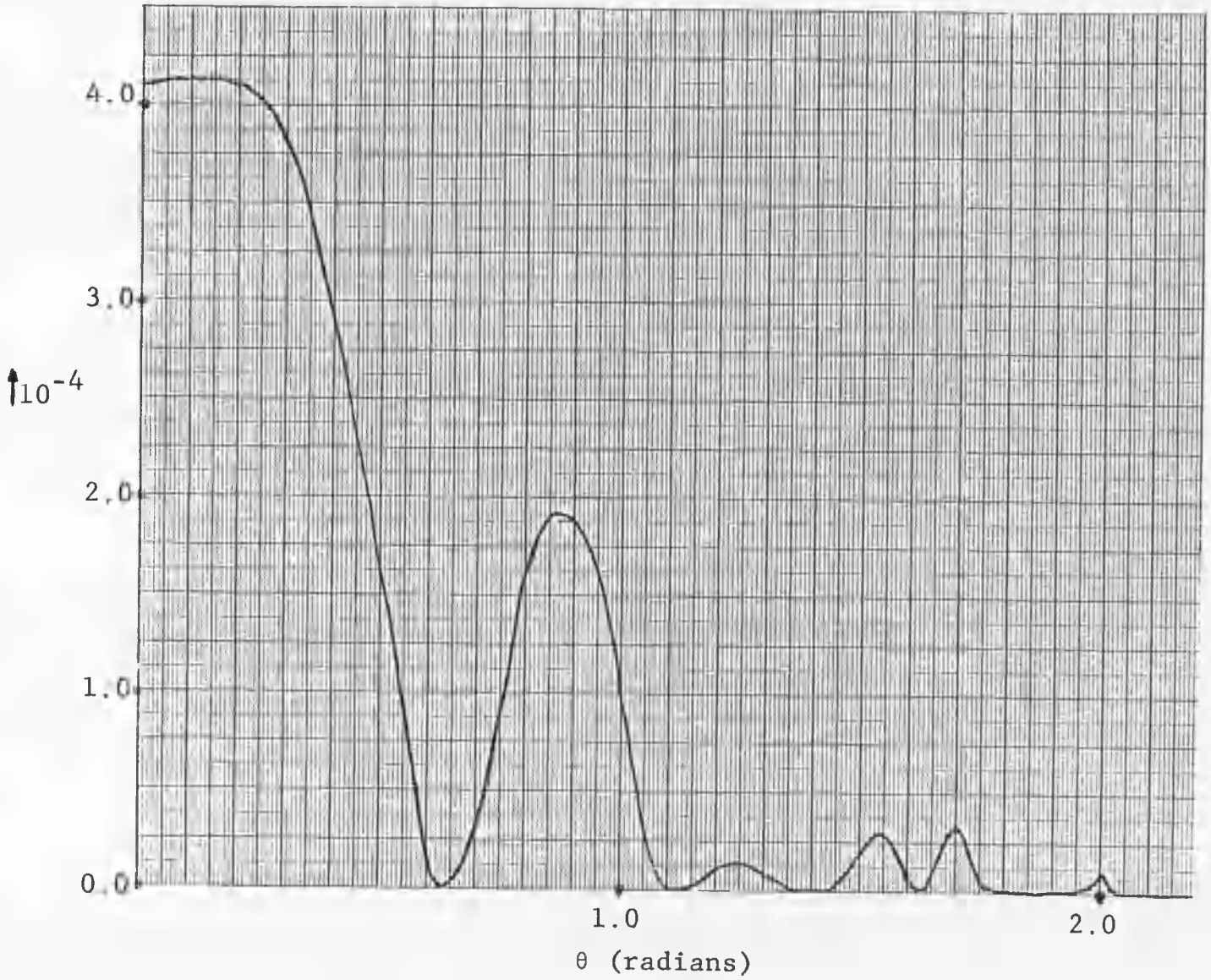

Figure 15. A graph of the integrand of $\mathrm{Im}[J_{11}(0.05,0.1)]$, for $\omega = \omega_2$.

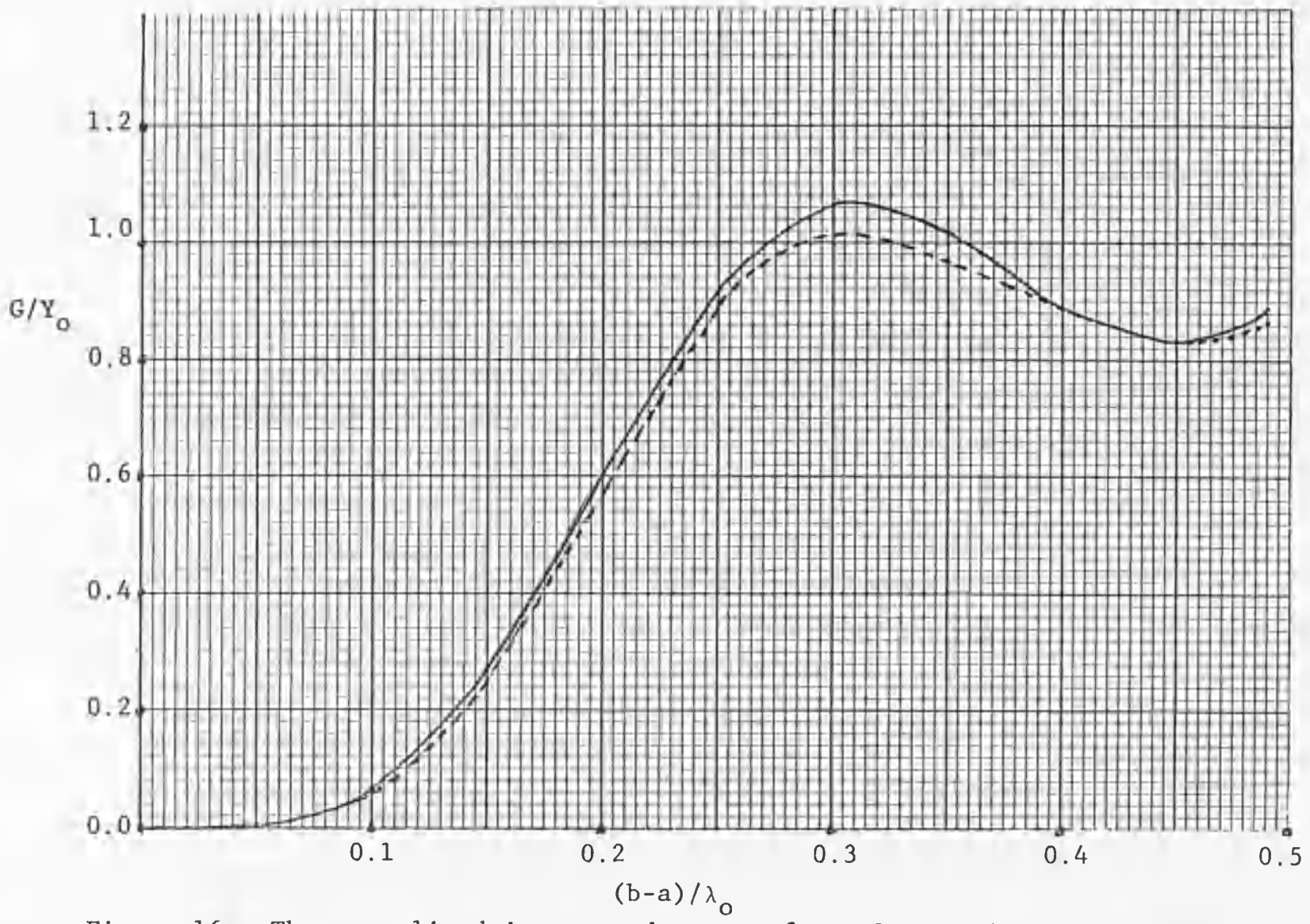

Figure 16. The normalized input conductance for only TEM (———) and including 30 higher order modes (-----). -- (———) taken from Marcuvitz 1951, p. 214.

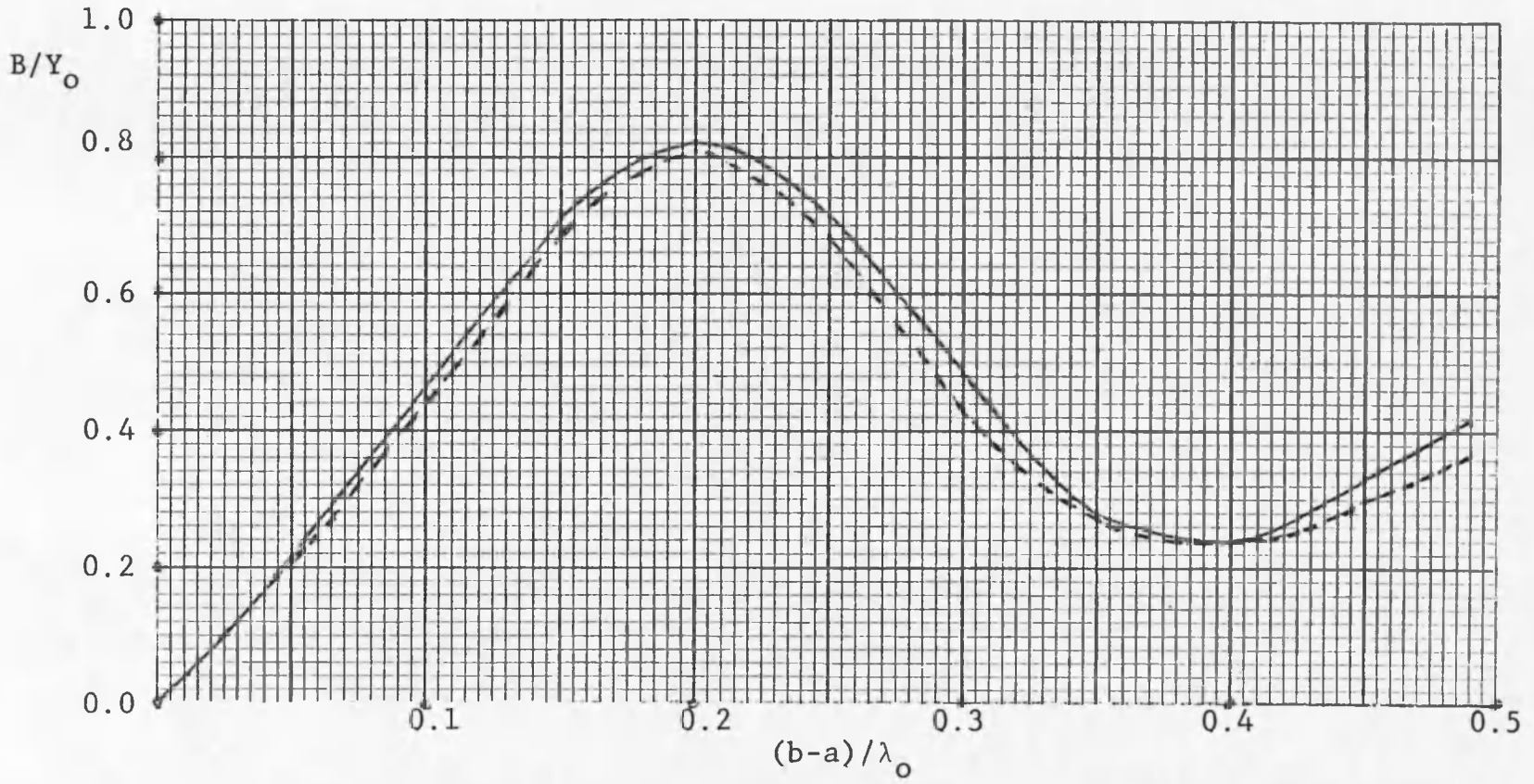

Figure 17. The normalized input susceptance for only TEM (———) and including 30 higher order modes (-----). -- (———) taken from Marcuvitz 1951, p. 215).

$$Y_o = \frac{2\pi}{\eta_1 \ln (b/a)}$$

The equivalent circuit at the input of the antenna is shown in Figure 18. The input admittance of the antenna was discussed by Levine and Papas (1951), Chang (1970), and Irzinski (1975), and a good agreement with their work is achieved.

The final part of the results to discuss here is the aperture fields. Figures 19 and 20 show plots of the magnitude of the radial component of the electric field vector at the aperture as a function ρ between $\rho = a$ and $\rho = b$. The convergence is rapid with N (the number of the TM modes considered). This is due to the small aperture considered $[(b-a)/\lambda_o = 0.67 \times 10^{-2}]$. We can see clearly from the plots that the major contribution of the higher order modes appear at $\rho = a$ and $\rho = b$. This is expected since they are the high frequency terms in the expansion. We also can see that the effect of the TEM part of the field on these plots varying as $1/\rho$. Since $Q_o'(\xi_n\rho)$ is the expansion function we expect higher frequency and lower intensity as the number of TM modes considered gets higher and this is clear also from the plots. At large n we showed in the previous chapter that:

$$Q_o'(\xi_n\rho) \tilde{=} \frac{2\cos(\xi_n(\rho-a))}{\pi\xi_n\sqrt{a\rho}}$$

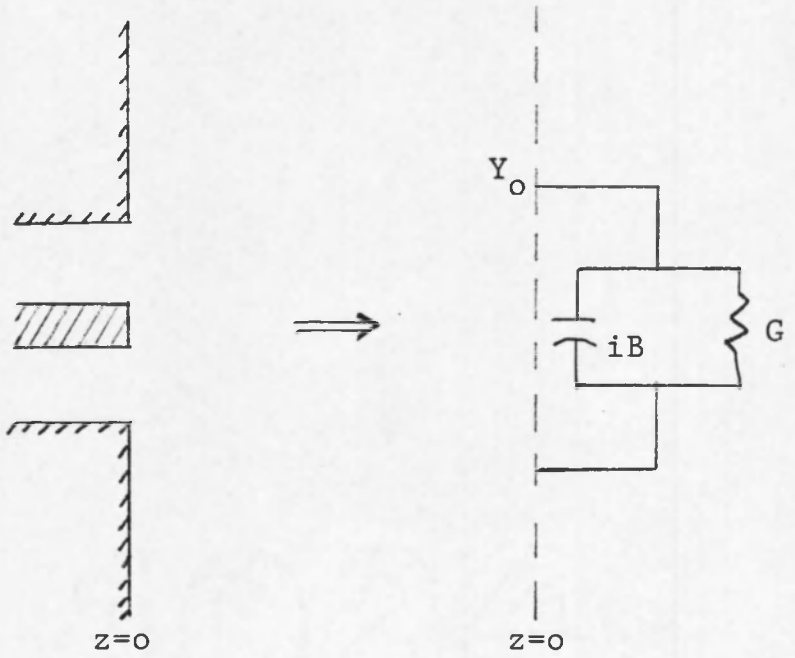

Figure 18. The input equivalent circuit.

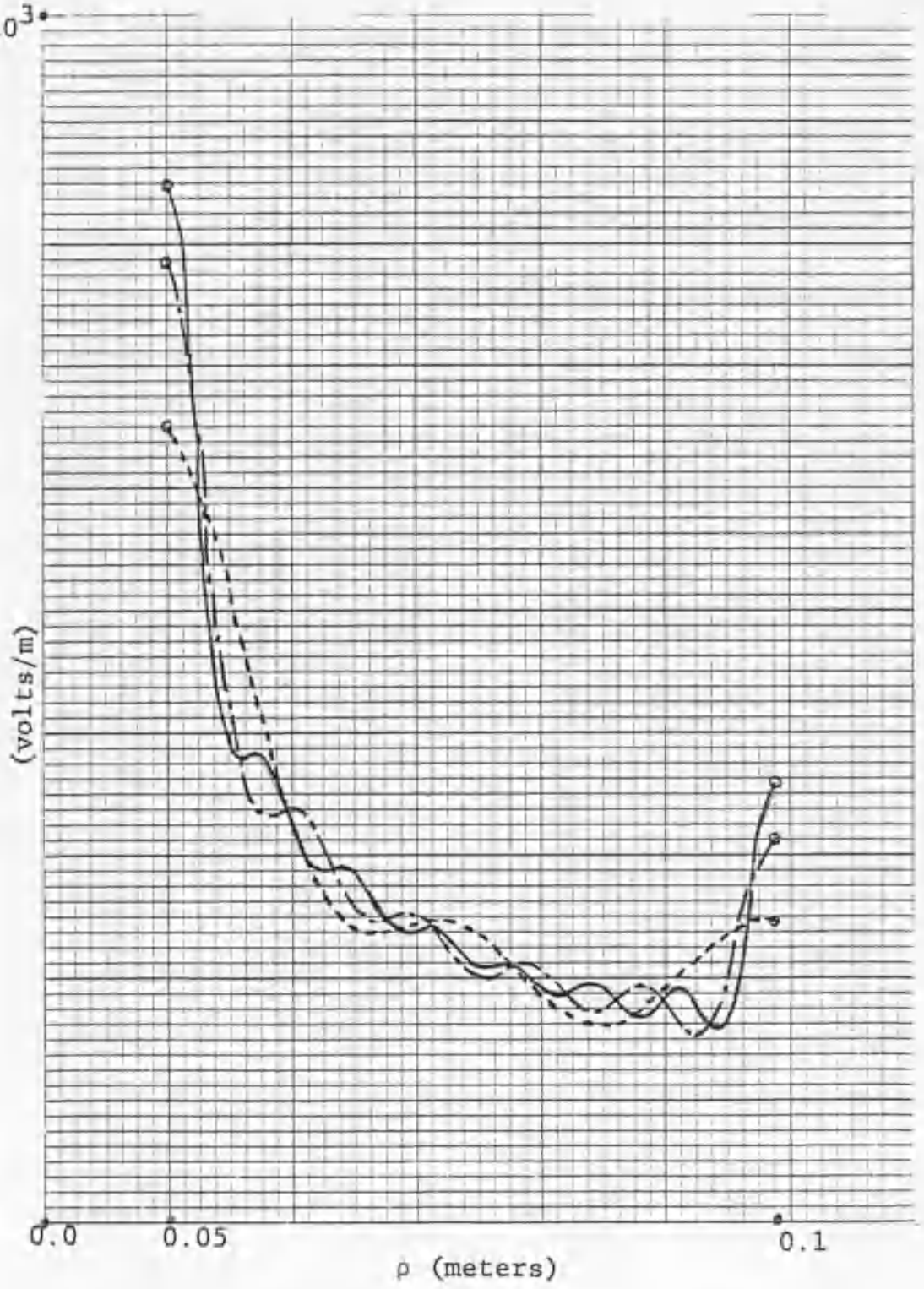

Figure 19. Electric aperture field [$E_{\rho_1}(\rho,o)$] for N=5 (-----), N=10 (-·-) and N=15 (———).

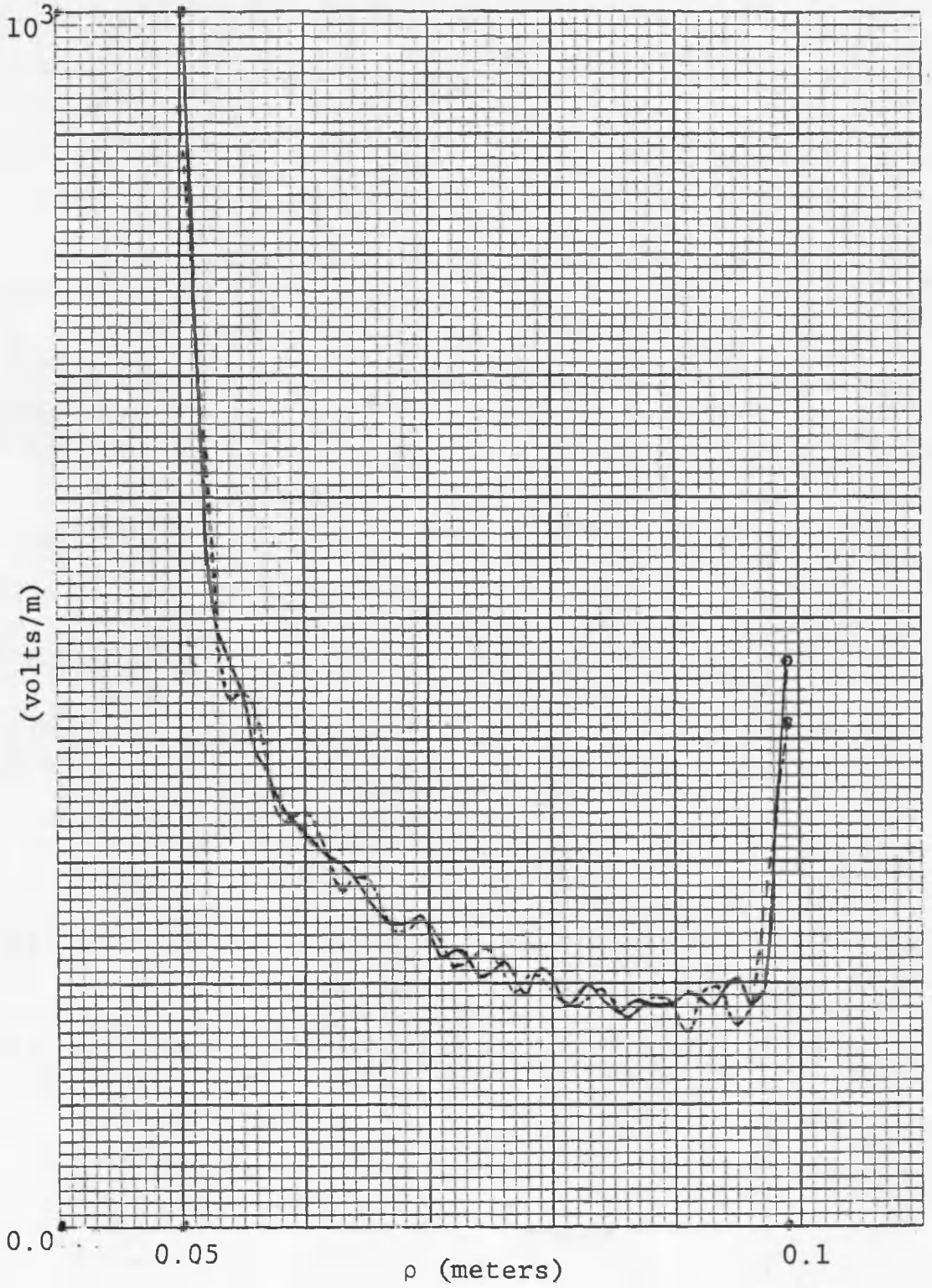

Figure 20. Electric aperture field [$E_{\rho_1}(\rho,o)$] for N=20 (-----) and N=30 (———).

from (5.8), we see that the field tends to be more oscillatory when ρ approaches b. This can be seen clearly on both Figures 19 and 20. One expects that the application of the edge discussed in the previous chapter will certainly smooth the graphs and emphasize the singularities at $\rho = a$ and $\rho = b$. From expression (5.8), the number of cycles m at any ρ is :

$$\xi_N(\rho-a) \tilde{=} \frac{N\pi(\rho-a)}{(b-a)} = 2m\pi$$

Therefore, the number of cycles made by $Q_o'(\xi_N \rho)$ from $\rho = a$ to $\rho = b$ is m such that:

$$m \tilde{=} N/2$$

We can see this clearly in the plots of Figures 19 and 20. Such oscillations are common in truncated Fourier series and are spurious. The argument of the radial component of the aperture electric field vector is not plotted, but it is found to be a constant from $\rho = a$ to $\rho = b$.

The absolute value of $H\phi_1(\rho,o)$ is plotted in Figure 21. From equation (2.11), we expect $H\phi_1(\rho,o)$ to be more rapidly converging than $E\rho_1(\rho,o)$ with the same number of TM modes considered. Figure 21 shows that the TEM part of is dominant and the effect of increasing N is affecting only at $\rho = a$ and $\rho = b$. The phase in this case is found constant from $\rho = a$ to $\rho = b$. At $\omega = \omega_2 = 2.79 \times 10^{10}$ radians per second $[(b-a)/\lambda_o = 0.74]$ the fields did not converge as rapid at N=30. Larger matrices are necessary and the use of

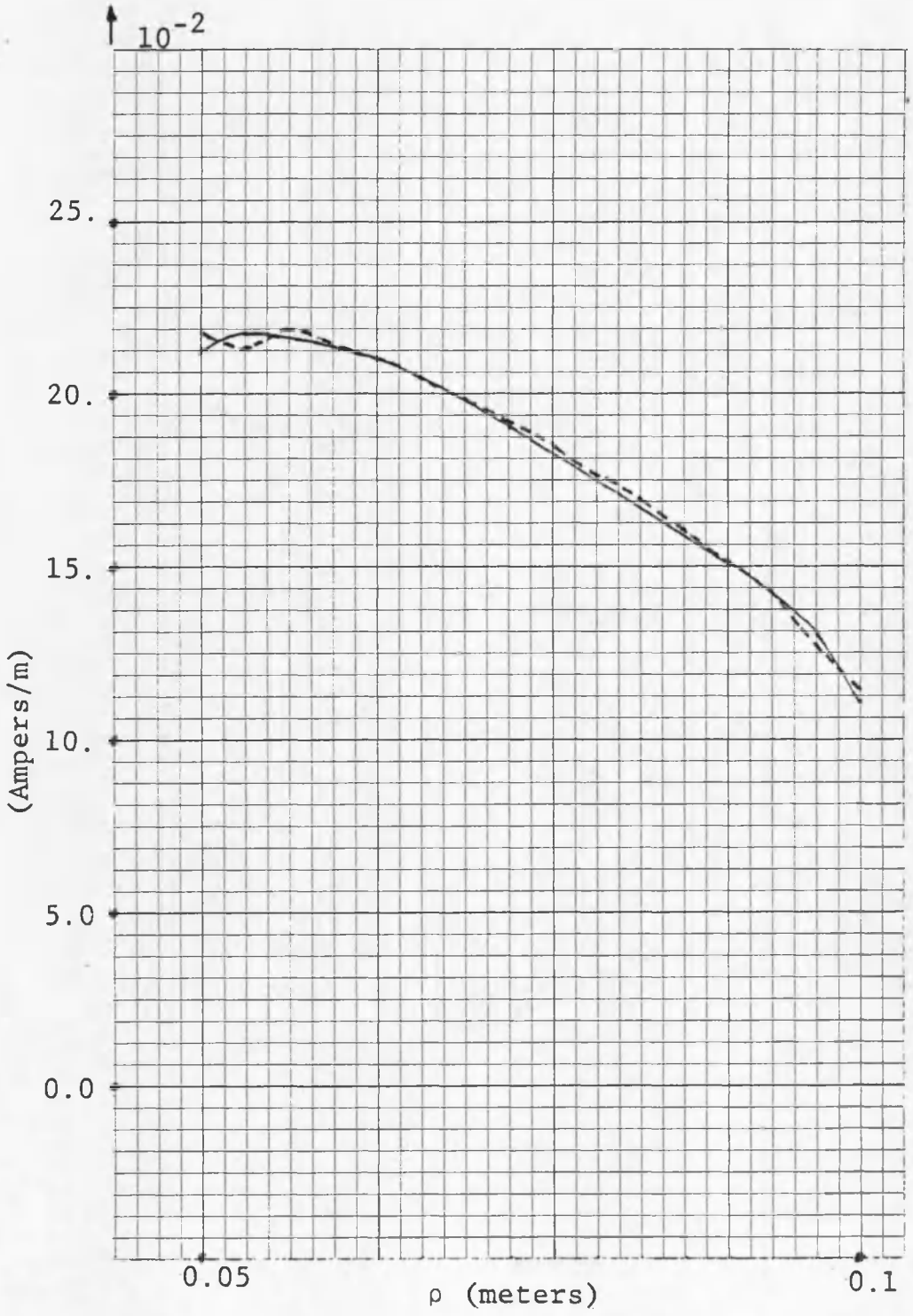

Figure 21. Magnetic aperture field for N=10 (-----) and N=30 (———).

the edge condition would improve convergence (Howard, 1972). Asymptotic behavior of the integrals discussed in Chapter 3 is also needed in this case.

CHAPTER 6

CONCLUSION

In conclusion, the use of the mode match method showed a good setting of the unknowns of this problem for numerical evaluation and the results obtained were satisfactory. Even though only an aperture of a small width was considered in the numerical results presented, the complete detailed analysis of the integrals in Chapter 3 assures good results for apertures of widths comparable to a wave length. The edge behavior application is needed in this case. Since the matrix L_{nm} is diagonally dominant, using a banded matrix ($n \tilde{=} m$) gives a good first approximation for it. This with the use of the efficient L-U decomposition matrix solving technique enables us to consider higher order matrix equations in the case of large apertures. As it was mentioned earlier, most of the computation time is taken in evaluating the integrals; so a worthwhile extension to this work will be to evaluate them using closed form contour integral techniques in the α-plane, or at least to derive asymptotic expressions to represent them for large n. One good extension to this problem is the case of excitation of finite structures or cavities where new boundary conditions will be

imposed by the structure. This is an important case since it arises when the center conductor is used as a measuring probe.

REFERENCES

Abramowitz, Milton, and I. A. Stegun, Handbook of Mathematical Functions, Dover Publications Inc., New York, 1970.

Chang, D. C., "Input Admittance and Complete Near-Field Distribution of an Annular Aperture Antenna Driven by a Coaxial Line," IEEE Trans. on Antennas and Propagation, AP-18, No. 5, pp. 610-616, 1970.

Cohn, G. I., and G. T. Flesher, "Theoretical Radiation Pattern and Impedance of a Flush-Mounted Coaxial Aperture," Proc. National Conf., 14, No. 2, pp. 150-168, 1958.

Copson, E. T., Asymptotic Expansions, Cambridge at the University Press, London, G. B., 1965.

Fitzgerrell, R. G., R. L. Gallwa, L. L. Haidle, A. Q. Howard, Jr., and J. E. Partch, "Buried Vertically Polarized UHF Antennas," Telecommunication Research Report No. 8, The U. S. Dept. of Commerce Publication, November, 1970.

Forsythe, G. E., and C. B. Moler, Computer Solution of Linear Algebraic Systems, Prentice-Hall, Englewood Cliffs, N. J., 1917.

Gradshteyn, I. S., and I. M. Ryzhik, Table of Integrals, Series and Products, Academic Press, New York, 1965.

Harrington, Roger F., Time-Harmonic Electomagnetic Fields, McGraw-Hill, New York, 1961.

Howard, A. Q., "On the Mathematical Theory of Electromagnetic Radiation from Flanged Waveguides," Journal of Math. Physics, pp. 482-490, 1972.

Irzinski, E. P., "The Input Admittance of a TEM Excited Annular Slot Antenna," IEEE Trans. on Antennas and Propagation, AP-23, No. 6, pp. 829-834, 1975.

Levine, H., and C. H. Papas, "Theory of Circular Diffraction Antenna," Journal of App. Physics, 22, No. 6, pp. 29-43, 1951.

Marcuvitz, N., Waveguide Handbook, Radiation Lab., M. I. T., Cambridge, Mass., 1951.

Meixner, J., "The Behavior of Electromagnetic Fields at Edges," IEEE Trans. on Antennas and Propagation, AP-20, No. 4, July, pp. 442-446, 1954.

Watson, G. N., A Treatise on the Theory of Bessel Functions, Cambridge University Press, Second Edition, 1958.